國立臺灣大學生物資源暨農學院生物科技研究所

碩士論文

Institute of Biotechnology

College of Bioresource and Agriculture

National Taiwan University

Master Thesis

PARP1 與 ZSCAN4 交互作用對端粒長度調節之探討

The Interaction Between PARP1 and ZSCAN4 and Their Roles on Telomere Regulation

蔡立廣

Li-Kuang Tsai

指導教授：宋麗英 博士

Advisor: Li-Ying Sung, Ph.D.

中華民國 108 年 8 月

August 2019

doi:10.6342/NTU201903408

國立臺灣大學碩士學位論文
口試委員會審定書

PARP1 與 ZSCAN4 交互作用對端粒長度調節之探討

The Interaction Between PARP1 and ZSCAN4 and Their Roles on Telomere Regulation

本論文係蔡立廣君（學號 R06642002）在國立臺灣大學生物科技研究所完成之碩士學位論文，於民國 108 年 7 月 22 日承下列考試委員審查通過及口試及格，特此證明。

口試委員：

（簽名）

（指導教授）

系主任、所長 （簽章）

doi:10.6342/NTU201903408

誌謝

轉眼間，碩士生活進入了尾聲。能夠如期畢業需要感謝許多人的協助。首先感謝指導老師 宋麗英老師在碩士生涯中給予我無數寶貴的建議，並提供很好的實驗室資源。感謝美國密西根大學的 徐捷博士在試驗設計與結果討論上大力的協助。感謝台灣大學動物資源中心 卓煥傑博士指導我邏輯性的思考、與我討論試驗結果並分享免疫沈澱的祕訣。也感謝口試委員 中國醫藥大學 朱志成老師；成功大學 楊尚訓老師；台灣大學 李宣書老師與林劭品老師在百忙中撥空指導。無論是口試時引導我思考試驗結果所代表的意涵並給予寶貴的建議，或是對於論文初稿之修改，都讓我更進一步地思考與學習，也讓本篇論文更加完善。

在實驗室生活中，首先必須感謝博士後研究員 張為芳博士從試驗設計、實驗技術到實驗室與鼠房之細節管理給予我近乎無微不至的細心指導。感謝 林姿穎學姊引領我了解實驗室大小事，並在聊天中讓我學習到正向思考的重要。感謝 彭敏學姊指導許多獨門技術，也見識到實驗可以如此快速。感謝 吳昀昕、徐淨、蔡一信（Alex)、吳虹霆，你們的陪伴讓實驗室充滿快活的氣氛，讓我得以面對實驗帶來的困難與挑戰。

感謝我的父母與家人，謝謝你們兩年來的支持與包容，讓我可以專注在實驗上，並順利取得學位。最後感謝 陳又嘉，能夠考取同一個研究所並一起為學位而努力是何其幸運，兩年來的陪伴與鼓勵是我完成學位功不可沒的力量！

doi:10.6342/NTU201903408

中文摘要

Zinc finger and SCAN domain containing 4 (*Zscan4*)為大量表現於二細胞時期鼠胚之基因。在體外培養中僅約1-5%的胚幹細胞可表達此基因。*Zscan4*之主要功能包含維持基因組穩定與調控端粒長度之動態平衡等，並可藉由非端粒酶之同源重組之方式延長端粒長度。然而，*Zscan4*延長端粒之分子機制至今仍未明瞭。透過免疫沈澱串聯質譜儀的方式，poly [ADP-ribose] polymerase 1 (PARP1)被預測為ZSCAN4潛在的結合蛋白之一，具有酵素活性，可將NAD^+上之ADP-ribose接至目標蛋白上。過去研究顯示PARP1為偵測DNA斷裂並參與在DNA修復之重要蛋白；更重要的是，剔除*Parp1*基因後，會導致小鼠端粒變短且提早老化。因此，本研究之目的為藉由探討ZSCAN4與其潛在結合蛋白PARP1之間的交互作用，以期進一步了解ZSCAN4延長端粒之機制。在本研究中，首先產製*Flag-Zscan4*與*Ha-Parp1*之重組質體，透過FLAG與HA抗體分別進行共同免疫沈澱，確認PARP1為一ZSCAN4之結合蛋白。接著，根據不同蛋白結構域將*Zscan4*與*Parp1*分別截斷為三個部分，包括*Zscan4*的SCAN、Linker sequence及Zinc finger （ZF) domain；與*Parp1*之DNA binding (DB)、Automodification (AM)及Catalytic domain，更進一步發現ZSCAN4以SCAN domain與PARP1之DB domain與AM domain結合，且ZSCAN4也會以ZF domain與PARP1之AM domain結合。為了解PARP1在ZSCAN4延長端粒中扮演之角色，進一步產製了ZSCAN4過表達之胚幹細胞株，並發現相較於控制組細胞，此細胞株之增殖速率較慢且端粒長度有較長的特性。接著，在施予PARP的抑制劑處理後，控制組胚幹細胞中發現端粒有顯著延長的現象；然在ZSCAN4過表達的胚幹細胞株中則觀察到細胞喪失其原本端粒長度較長的特性，顯示PARP1可能在ZSCAN4延長端粒的機制中扮演著雙重的角色。後續以短髮夾RNA降低*Parp1*的表現量後，觀察到端粒調控相關之基因被激活，*Zscan4*的表現量有顯著的提升，且端粒有延長的現象，進一步證實了PARP1具有抑制*Zscan4*表現的能力。最後透過端粒酶半缺失（$Terc^{+/-}$）之核移殖胚幹細胞（ntESCs）模擬端粒綜合症的患者，施予PARP的抑制劑，期能補救其端粒較短之缺陷。結果顯示，試驗之三株$Terc^{+/-}$ ntESCs中，其中一株ntESCs有顯著延長端粒的效果。綜上所述，本研究驗證PARP1為一與ZSCAN4結合之蛋白，並進一步揭露其交互作用之蛋白功能域；另也發現PARP1在調控ZSCAN4與端粒長度上可能扮演著雙重的角色，然而*Zscan4*如何參與延長端粒更詳盡之分子機制仍待更進一步的實驗釐清。由於*Zscan4*為藉由非端粒酶途徑調控端粒長度之重要蛋白，若能深入探討*Zscan4*延長端粒之分子機制，盼能為端粒綜合症患者提供有效治療之策略或方向。

關鍵詞：ZSCAN4、PARP1、端粒、胚幹細胞

doi:10.6342/NTU201903408

ABSTRACT

Zinc finger and SCAN domain containing 4 (*Zscan4*) is a gene that expressed in 2-cell stage embryos and sporadically in a subpopulation of embryonic stem cells (ESCs). *Zscan4* participates in the regulation of telomere homeostasis and genomic stability. However, the detailed mechanism of *Zscan4* involved in telomere elongation is still unclear. Poly [ADP-ribose] polymerase 1 (PARP1) is known to sense DNA damage and activate several DNA repair pathways. The objective of this study is to investigate the mechanisms of PARP1 interacts with ZSCAN4 and participates in telomere regulation. By serial immunoprecipitations, our data showed that PARP1 not only interacted with SCAN domain of ZSCAN4 through DNA binding domain and auto-modification domain but also interacted with zinc finger domain of ZSCAN4 by auto-modification domain. To investigate whether PARP1 is associated with ZSCAN4 in telomere homeostasis, *Zscan4* over-expressed ESCs (OEZ4 ESCs) were generated. We found that OEZ4 ESCs show slower proliferation rate and significantly longer telomere length compared to the vector control. Moreover, inhibition of PARP1 activity by treating 3-aminobenzamide (3-AB), the PARP inhibitor, led to shorten telomeres in OEZ4 ESCs, indicating PARP1 may play dual roles to interact with *Zscan4* and participates in telomere regulation. Next, knockdown *Parp1* by shRNA in ESCs showed elongation of telomere length and activation of genes involved in telomere regulation, suggesting PARP1 regulates telomere homeostasis. Lastly, treating 3-AB in $Terc^{+/-}$ ntESCs, which mimic the telomere syndrome patient, we further reveal that shorten telomeres has been elongated. In conclusion, this study uncovers PARP1 as a ZSCAN4-associated protein and participates in telomere regulation, and provides novel insights on the molecular interaction between DNA damage and telomere regulation.

Keyword: ZSCAN4, PARP1, telomere, embryonic stem cells

doi:10.6342/NTU201903408

CONTENTS

doi:10.6342/NTU201903408

doi:10.6342/NTU201903408

LIST OF FIGURES

doi:10.6342/NTU201903408

LIST OF TABLES

doi:10.6342/NTU201903408

ABBREVIATIONS

Full name	Abbreviations
3-aminobenzamide	3-AB
Alternative lengthening of telomere	ALT
Ataxia telangiectasia and Rad3-related kinase signaling	ATR
Ataxia telangiectasia mutated kinase signaling	ATM
ATRX chromatin remodeler	Atrx
Break-induced replication pathway	BIR
Cytosine-rich extrachromosome circle	C-circle
Dimethyl sulfide	DMSO
DNA (cytosine-5)-methyltransferase 3B	*Dnmt3b*
DNA damage response	DDR
DNA double strand break	DSB
Double homeobox 4	*Dux4*
Embryonic stem cells	ESCs
Homologous recombination	HR
Mitosis DNA synthesis	MiDAS
Murine endogenous retrovirus with leucine tRNA primer	*MERVL*
Non-homologous end joining	NHEJ
Poly [ADP-ribose] polymerase 1	*Parp1*
Protection of telomere 1	POT1
Regulator of telomere elongation helicase 1	*Rtel1*
Replication timing regulatory factor 1	*Rif1*
Repressor / Activator protein 1	RAP1
Short hairpin RNA	shRNA
Suppressor of variegation 3-9 homolog 2	*Suv39h2*
T-box transcription factor	*Tbx3*
Telomerase reverse transcriptase	*Tert*
Telomerase RNA component	*Terc*
Telomere maintenance 2	*Telo2*

doi:10.6342/NTU201903408

Full name	Abbreviations
Telomere sister chromatin exchange	T-SCE
Telomere-loop	T-loop
Telomere/ single copy gene ratio	T/S ratio
Telomeric repeat-binding factor 1	TRF1
Telomeric repeat-binding factor 2	*Trf2*
TRF1- and TRF2- interacting nuclear protein 2	TIN2
Tripeptidyl-peptidase 1	TPP1
Zinc finger and SCAN domain containing 4	*Zscan4*

doi:10.6342/NTU201903408

CHAPTER I:

GENERAL INTRODUCTION AND LITERATURE REVIEW

doi:10.6342/NTU201903408

1. GENERAL INTRODUCTION

Telomeres are tandem repeated sequence at the end of chromatin which can prevent chromosome end-to-end fusion and maintain genome stability. The telomere sequence is “TTAGGG” both in human and mouse. In most of cells, telomeres shorten after DNA synthesis due to DNA polymerase characteristics. More specifically, it is necessary to have a polynucleotide to act as primer for DNA polymerase to start DNA synthesis, while exonuclease cuts the polynucleotides primer after DNA synthesis (Baltimore and Smoler, 1971; Allsopp et al., 1995). However, in highly proliferating cells, such as: germ cells, embryonic stem cells (ESCs) and cancer cells, telomeres can be elongated by telomerase or alternative lengthening of telomeres (ALT) pathway (Bryan et al., 1995; Shay and Bacchetti, 1997).

At the telomere, several proteins form the shelterin structure and circularize telomere into telomere loop (T-loop), which can protect chromosome from being recognized as DNA double strand breaks (DSBs). DSB pathway will be activated after telomere shortening (Doksani and de Lange, 2016; Lazzerini-Denchi and Sfeir, 2016). DNA DSB can be repaired by either non-homologous end joining (NHEJ) or homologous recombination (HR) pathways (Mehta and Haber, 2014). Among them, the ALT pathway is classified to HR pathway (Arora and Azzalin, 2015). For sensing the DNA lesion, PARP1 sensed and localized to the DNA break sites earlier than other DSB sensors (Yang et al., 2018).

A subpopulation of ESCs have expressed 2-cell stage embryo-specific genes (2-cell genes) including, *Zinc finger and SCAN domain containing 4* (*Zscan4), murine endogenous retrovirus with leucine tRNA primer (MERVL), double homeobox 4 (Dux4)* and so on. is one of the 2-cell genes which can increase the telomere sister chromatin

doi:10.6342/NTU201903408

exchange rate (T-SCE) then elongated telomere length by ALT pathway (Falco et al., 2007; Dan et al., 2017). However, the mechanism of *Zscan4* participates in telomere regulation is still unclear.

Since telomere length affects potency and differentiation of pluripotent stem cells (Sung et al., 2014; Aguado et al., 2017), investigating molecular mechanism of Zscan4, the protein mainly expressing in pluripotent stem cells and responsible for telomere elongation, may provide useful information for studying the stemness of ESCs.

doi:10.6342/NTU201903408

2. LITERATURE REVIEW

2-1. Functions of telomere

Telomeres are the tandem repeated sequence at the end of linear chromatin in eukaryotic cells. In the mouse and human, the sequence is TTAGGG. Thanks to telomere sequence and the end structure, DNA avoid from end-to-end fusion, genome instability and being recognized as DNA damage (Lewin *et al*., 2014). Precisely, there are 6 core proteins form shelterin, specifically binding to telomere, including TRF1, TRF2, TIN2, TPP1, POT1 and RAP1. Telomeres have G-rich single strand ends, with the help of shelterin, the end invades into double strand forms so-called T-loop. The T-loop structure prevents telomere from DNA fusion (Lazzerini-Denchi and Sfeir, 2016). Among shelterin subunits, TRF1 and TRF2 are responsible for binding with double stand DNA. TIN2 interacts with both TRF1 and TRF2 and also binds with TPP1/POT1 heterodimer. POT1 is critical for it characteristic of binding with single strand DNA. Shelterin inhibits DNA damage response (DDR). Without shelterin, DDR will be activated, followed by p53 expression and apoptosis or senescence (Ferron et al., 2004; Sperka et al., 2011). For example, TRF2 and POT1 independently inhibit ataxia telangiectasia mutated (ATM) kinase signaling and ataxia telangiectasia and Rad3-related (ATR) kinase signaling, respectively (Denchi and de Lange, 2007). Second, shelterin and Ku complex inhibit alternative-NHEJ pathway (alt-NHEJ, Cheng et al., 2011; Lazzerini-Denchi and Sfeir, 2016).

doi:10.6342/NTU201903408

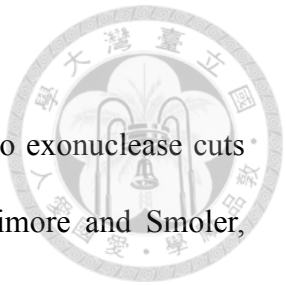

2-2. Ways to elongate telomere length

Telomeres progressively shorten after DNA replication due to exonuclease cuts the primer region of DNA polymerase after DNA synthesis (Baltimore and Smoler, 1971; Allsopp et al., 1995). There are 2 distinct ways to elongate telomeres: telomerase dependent pathway and alternative lengthening of telomere pathway (Cesare and Reddel, 2010).

In most of somatic cells, the activity of telomerase is repressed (Ulaner et al., 1998). Telomerase only expresses in highly proliferating cells. In mammals, telomerase is mainly formed by telomerase reverse transcriptase (TERT) associates with a telomerase RNA component (TERC, Greider and Blackburn, 1985). TERC is the repeated telomere-complementary RNA sequence. TERT uses TERC as a template to bind with telomere sequence, and then does the reverse transcription. TERT shifts from 5' to 3' to repeatedly elongate telomere (Sarek et al., 2015). Finally, DNA polymerase adds complementary sequence from 3' to 5' to form DNA double strands.

Except for telomerase, cells can also use ALT pathway to elongate telomere. In 1995, Bryan et al firstly described telomere elongation without detectable telomerase activity (Bryan et al., 1995). 2 years later, Bryan et al named this mechanism as alternative lengthening of telomere (Bryan et al., 1997). ALT-elongated telomere has several phenotypes, including: 1) variation in telomere length; 2) increase rate of T-SCE; 3) formation of telomere circle; 4) formation of extrachromosomal telomere repeats and 5) formation of ALT-associated promoelocytic leukemia protein nuclear bodies (APBs, Bryan et al., 1995; Lazzerini-Denchi and Sfeir, 2016; Zhang et al., 2019). The detail mechanism of ALT pathway is still unclear. In tumor cells, ALT pathway is activated as a result of p53/ATRX/DAXX/H3F3A mutation or telomerase suppression.

doi:10.6342/NTU201903408

It has been proven that inhibition of factors involved in HR pathway (RAD51, MRN, RAD9, RAD17 and RPA) results in ALT been repressed. This result points out that HR pathway is required for ALT (Gocha et al., 2013). T-SCE, one of the famous ALT phenotypes, can be repressed by the Ku complex and multiple shelterin subunits, including TRF2, RAP1 and POT1 (Lazzerini-Denchi and Sfeir, 2016). In ESCs, ZSCAN4 is found to have ability to increase T-SCE rate (Dan et al., 2017).

Recently, reports indicated that ALT pathway was occurred through break-induced replication pathway (BIR, Min et al., 2017; Zhang et al., 2019). In *Terc* knockout human cells, Min et al discovered that ALT positive cells are easy to have telomere replication problem because G-rich sequence forms G-quadruplexes structure in telomere region. The problem result in trigger mitosis DNA synthesis (MiDAS) at telomere. MiDAS is processed by BIR, a kind of HR pathway (Min et al., 2017). Unlike HR occurred at other DNA site is mostly dependent on Rad51, the ALT at telomere is Rad51 independent and can be divided into Rad52 dependent and Rad52 independent sub-pathways. Furthermore, Rad52 is required to maintain telomere length. However, Cytosine-rich extrachromosome circle (C-circle), a hallmark of ALT, forms through Rad52 independent pathway (Zhang et al., 2019).

It has been reported that cell may repair stalled replication fork switch from error-free HR pathway to error-prone NHEJ pathway. For example, stalled replication fork could be repaired by BIR pathway and then switch into alt-NHEJ pathway (Hastings et al., 2009; Ottaviani et al., 2014). Since alt-NHEJ pathway dependents on micro-homologous sequence (2-15 bp of complementary sequence), it is reasonable to occur at repeated sequence, such as telomere.

doi:10.6342/NTU201903408

2-3. Zinc finger and SCAN domain containing 4 (ZSCAN4)

ESCs are known for their heterogenous gene expression profiles. Within ESCs, there are a subpopulation that has the gene expression profile similar as 2-cell stage embryos, so-called 2 cell-like ESCs (2C-ESCs). Unlike the pluripoency of general ESCs, 2C-ESCs are transient totipotent, which have the ability to differentiate to not only all 3 germ layer but also extraembronic tissues including yolk sac and placenta (Macfarlan et al., 2012). ESCs enter 2-cell-like state regularly and also depend on intrinsic and extrinsic factors, like: oxidative level or culture medium. Normally, each cell in and out of 2 cell-like state within 17 passages (Macfarlan et al., 2012). 2C-ESCs show lower pluripotent marker expression, translation block and hypomethylation. 2C-ESCs can be identified by MERVL positive and ZSCAN4 positive populations (Eckersley-Maslin et al., 2016).

Zscan4 is the gene firstly discovered at 2007, as a gene only expressed in 2-cell stage embryos and 2C-ESCs. In mouse, *Zscan4* has 6 paralogs with 3 open reading frames, which are *Zscan4c*, *Zscan4d* and *Zscan4f*. *Zscan4c* major expresses in 2 cell-like ESCs while *Zscan4d* major expresses in 2-cell stage embryos. *Zscan4* is been strictly regulated in early embryo development. For example, knockdown or consistently expression of *Zscan4* in zygote leads to hatching and implantation failure. In *in vitro* culture, *Zscan4* knockdown or consistently expressed results in lower percentage of blastocyst outgrowth compare to control (Falco et al., 2007). In ESCs, only 1-5% of cells expressed *Zscan4* at any given time. Yet, nearly all cells expressed *Zscan4* once within 9 passages. *Zscan4* has ability to elongate telomere caused by increase T-SCE rate (Zalzman et al., 2010). *Zscan4* may directly regulate telomere length since exogenous *Zscan4* colocalizes with telomere at M phase (Zalzman et al.,

doi:10.6342/NTU201903408

2010). Or, ZSCAN4 may act as transcription factor because activation of *Zscan4* changes expression level of ~1000 genes (Nishiyama et al., 2009). *Zscan4* is activated in short telomere with extended cell cycle (Nakai-Futatsugi and Niwa, 2016). Furthermore, most of ZSCAN4 positive cells are at late S to G2 phase in cell cycle. Notably, arrested cell cycle at G2/M phase by nocodazole do not increase *Zscan4* expression level (Storm et al., 2014). Additionally, *Zscan4* activated transient expression of eukaryotic translation initiation factor 1A (*Eif1a*)-like genes lead to globally repressed of protein synthesis (Hung et al., 2013).

In ESCs, Zscan4 positive cells show derepression of heterochromatin. This is associated with increase of activated histone modification, many heterochromatin have been activated, including centromere, telomere and endogenous retroviruses regions (Akiyama et al., 2015). This result suggests that *Zscan4* dramatically affects epigenetics in ESCs. It has been reported that ZSCAN4 binds with DNMT1 and UHRF1, induces UHRF1 dependent ubiquitination then finally leads to DNMT1 degradation and global hypomethylation (Dan et al., 2017). In the 2C-ESCs, TBX3 inhibits DNMT3B binding to telomere region and *Zscan4* promoter results in *Zscan4* activation and hypomethylation (Dan et al., 2013). Besides, ZSCAN4 is found to be interacting with LSD1 (also known as KDM1A), the protein responsible for demethylation of H3K4 and H3K9 mono-and dimethylation (Storm et al., 2014). On the other hand, histone acetylation also affect Zscan4 expression and telomere length. Treatment of histone deacetylase (HDAC) inhibitor in ESCs induced numerous 2-cell genes expression, including *Zscan4* (Dan et al., 2015).

Since 2C-ESCs have transient totipotency, ZSCAN4 has also been reported to be involved in regulation of differentiation potency. In 2012, Zscan4 was reported could

doi:10.6342/NTU201903408

efficiently generate induced pluripotent stem cells (iPSCs) when co-expressed with Klf4, Oct4, and Sox2 (Hirata et al., 2012). Interestingly, iPSCs generated by Zscan4, c-Myc, Klf4, Oct4, and Sox2 (ZMKOS) have better karyotypes than iPSCs generated by conventional MKOS (Hirata et al., 2012). Activation of *Z*scan4 by tet-on system can restore ESCs developmental potency. In the study, by tetraploid (4N)-blastocyst complementary assay, the group shows that force expression of *Z*scan4 can increase ESCs potency in long term cell culture (from passage 12 to passage 48). Moreover, by injected single *Z*sacn4-positive ESC into 4N blastocyst, Zscan4 positive group shows higher live embryos rate than control (5% v.s. 0%, Amano et al., 2013).

2-4. Poly (ADP-ribose) polymerase 1 (PARP1)

Parp1 is a protein with DNA binding and poly ADP-ribosylation (PARylation) characteristics. *Parp1* has 3 major domains, including: DNA binding domain (1-382 a.a.), auto-modification domain (383-655 a.a.) and catalytic domain (655-1014 a.a., Cepeda et al., 2006). With DNA binding domain, PARP1 has an ability to binding with DNA. Moreover, PARP1 is one of the first DSB sensor which directly binds to DSB site (Rouleau et al., 2010; Yang et al., 2018). After binding with DSB site, PARP1 transiently recruits various proteins to repair DSBs by multiple DNA Repair pathways (Rouleau et al., 2010). Most importantly, PARP1 plays a critical role in alternative NHEJ pathway (alt-NHEJ).

Alt-NHEJ is a Ku-independent pathway while classical-NHEJ is a Ku-dependent pathway. Alt-NHEJ has also been called micro homology end join (MMEJ). In alt-NHEJ pathway, 5-25 bp of micro homologous sequence near DSB ends be recognized and anneal to each other. alt-NHEJ is an error-prone pathway (McVey and Lee, 2008). It

doi:10.6342/NTU201903408

has been proven that PARP1 involves in non c-NHEJ pathway through recognizing-connecting DNA ends and recruits XRCC1/DNA ligase 3 for ligation (Audebert et al., 2004; Frit et al., 2014). Furthermore, PARP1 is required for alt-NHEJ and PARP1 inhibitor can act as radiosensitizer in tumor therapy (Kotter et al., 2014).

PARP1 also participates in telomere specific DNA repair or elongation. PARP1 is proven binding with TRF2, one key component of shelterin. Also, PARP1 shows it ability, as DNA damage sensor, to bind with erode telomere after H_2O_2 treatment (Gomez et al., 2006). In artificial telomere internal break which is induced by Fok1-TRF1 fusion protein, the DSB can be repaired by PARP1/Lig3 dependent alt-NHEJ pathway or HR pathway (Doksani and de Lange, 2016). In mouse fibroblast cell line, inhibition of PARP1 enzyme activity leads to telomere elongation through ATM pathway in long term culture (48-52 population doubling), while the same group reported the similar result in human cell line with the unaffected of telomerase activity data (Lee et al., 2015). In addition, PARP1 inhibition activates ATM pathway. The results imply that PARP1 inhibition elongated telomere through telomerase independent pathway, the ALT pathway. On the other hand, Hsieh *et al* discovered that PARP1 recruits KLF4 to activated the expression of *Tert*, the component of telomerase. In mouse ESCs, polymerase enzyme activity of PARP1 is required for telomerase activity (Hsieh et al., 2017). However, chronic inhibition of PARP1 shows telomere shorten in human fibroblast with slower proliferation rate and subtelomeric region DNA methylation level decrease (Boesten et al., 2013). Also, knockout of *parp1* shows shorter telomere and accelerates aging both *in vitro* and *in vivo* in mouse model (d'Adda di Fagagna et al., 1999; Piskunova et al., 2008). In summary, effect of PARP1 on

doi:10.6342/NTU201903408

telomere length may depend on dosage and duration of inhibitor, while PARP1 is certainly involved in telomere length regulation.

PARP1 also affects cell potency. It has been reported that pluripotent stem cells express more *parp1* than MEFs. During Oct4/Sox2/Klf4/c-Myc induced reprogramming, inhibition of PARP1, by either shRNA or chemical, reduce iPSCs generation efficiency. Moreover, PARP1 has an ability to replace *Klf4* or *c-Myc* to generate chimera-accessible iPSCs. Oct4/Sox2/Parp1-iPSCs have even higher efficiency of iPSCs generation than Oct4/Sox2/Klf4 or Oct4/Sox2/c-Myc derived iPSCs (Chiou et al., 2013). By immunoprecipitation, PARP1 shows protein-protein interaction with KLF4, a key reprogramming factor. Knockdown of PARP1 not only decreases the expression of pluripotent markers, such as: *Oct4*, *Sox2* and Rex1 but also has more tendency of differentiation (Roper et al., 2014; Hsieh et al., 2017). More specifically, *Parp1* affects reprogramming and pluripotency through its function of PARylation (Jiang et al., 2015). Also, in 2014 PARP1 is predicted to be binding to *Zscan4* promoter in HEK293T cells (Lodhi et al., 2014).

2-5. Effect of telomere length on stem cells potency

The telomere length not only affects genome stability but also affect stem cells potency and differentiation. ESCs with short telomeres show lower efficiency on generation of germ line-competent chimera pups while iPSCs with short telomeres have decrease ability to generate teratoma (Huang et al., 2011). *Terc* insufficient nuclear transfer ESCs (ntESCs) failed to produce live pup in 4N-blastocyst complementation assay, the most strictest test of ESCs potency (Sung et al., 2014). Besides, iPSCs with short telomeres have more tendency to differentiate to ectoderm (Aguado et al., 2017).

doi:10.6342/NTU201903408

Moreover, *Terc* knockout ntESCs show chondrogenesis defect (Chang et al., 2019). These results indicate that telomere length is critical for stemness of pluripotent stem cells.

3. PERSPECTIVE

Telomere is often thought to be the guardian of chromatin, which can protect linear chromatin from chromatin fusion and genome instability. Due to characteristics of DNA polymerase, telomere is shorten after DNA replication. There are two distinct ways to elongate telomere: telomerase-dependent pathway and telomerase-independent ALT pathway. Although ALT pathway has been reported as one branch of BIR pathway, it is still unclear about detailed mechanisms of ALT pathway.

ESCs have heterogenous gene expression profile. In the ESCs, cells in and out of so-called "2-cell state" to elongate telomere and have transient totipotency (Macfarlan et al., 2012). Expression of *Zscan4* acts as a hallmark of 2-cell state ESCs. ZSCAN4 has ability to increase T-SCE, one phenotype of ALT pathway, then elongates telomere (Dan et al., 2017). However, little is known about molecular mechanisms of *Zscan4*.

Zscan4 has been reported to be involved in pluripotency, epigenetic and telomere homeostasis. However, the specific mechanism of *Zscan4* is still unclear. In the previous study, by the mass spectrum, PARP1 is predicted to have protein interaction with ZSCAN4 (Sung et al., unpublished data). Thus, in this study, I aim to investigate whether PARP1 and ZSCAN4 indeed have protein-protein interaction, also, whether PARP1 participates in Zscan4 induced telomere elongation. Firstly PARP1 is identified as a ZSCAN4 associated protein. Secondly, by produced truncated ZSCAN4

doi:10.6342/NTU201903408

and PARP1, we further examine the interaction domains of these two proteins. Lastly, I tried to explore whether PARP1 involves in telomere regulation with Zscan4. Since telomere length is known to be critical for ESCs potency. These finding provide more information to the telomere elongation mechanism of *Zscan4*, the protein responsible for telomere elongation, may contribute to investigate stemness of ESCs.

doi:10.6342/NTU201903408

CHAPTER II:

VERIFICATION OF PARP1 INTERACTS WITH ZSCAN4

doi:10.6342/NTU201903408

1. BACKGROUND

In 2007, Zinc finger and SCAN domain containing 4 (*Zscan4*) is firstly be discovered as a novel gene only expressed in 2 cell stage embryo and a subpopulation of embryonic stem cells (ESCs). Zscan4 is highly regulated, and either knockdown or over-expression of Zscan4 leads to implantation failure (Falco et al., 2007). Within these years, Zscan4 is famous for its ability to elongate telomere through alternative lengthening of telomere (ALT) pathway, which is a telomerase independent pathway. However, how ZSCAN4 extensively affects cell physiology is still unclear. Therefore, here, I investigate mechanisms of ZSCAN4 participate in telomere length regulation from its associated candidate, poly-ADP ribose polymerase 1 (PARP1).

PARP1 is well-known for its ability to sense DNA breaking site and activates several DNA repair pathway. PARP1 has ability to post-translationally modify its targets by ADP-ribose. The protein ADP-ribosed by PARP1 may lead to numerous results: 1) gene regulation by affected DNA binding of target protein. 2) recruitment of target to repair DNA. 3) Protein degradation.

Most of the functional domains are conserved between proteins or even species. ZSCAN4 can be truncated into SCAN domain, Linker sequence and Zinc finger domain (Dan et al., 2017). SCAN domain is a conserved ~80 residues motif with leucine-rich region. SCAN domain is predicted to be α-Helices. SCAN domain is usually at N-terminal of protein with Cys2-His2 (C2H2) type of Zinc finger motif at C-terminal. The protein with SCAN domain may serve as a transcription factor. SCAN domain is responsible for self-association or association of other proteins (Williams et al., 1999; Edelstein and Collins, 2005). For example, ZSCAN4 forms dimer through SCAN domain (Dan et al., 2017). Zinc finger domain can be further classified into several

doi:10.6342/NTU201903408

categories. ZSCAN4 has 4 C2H2 type zinc finger motif. C2H2 type zinc finger motif has been reported to bind with DNA, RNA, lipid or protein (Vilas et al., 2018). For example, ZSCAN4 interacts with UHRF1 via Zinc finger domain (Dan et al., 2017). On the other hand, PARP1 can be divided into 3 parts: DNA binding domain (DBD), auto-modification domain (AMD) and catalytic domain (CD, Cepeda et al., 2006). In DBD it has 2 Zinc finger motifs which have ability to bind with DNA. also, the Nuclear localization signal of *Parp1* is located in DBD as well. The central part, AMD, is the site for PARP1 to accept ADP-ribose. After PARP1 be ADP-ribosylation, PARP1 is inactivated. Also, PARP1 senses and binds to DNA breaking site as a holo-dimer while AMD serves as dimer forming site. At the C-terminal is the CD domain, which is conserved between PARPs and is the site have enzyme activity. CD is responsible for binding to target proteins and hydrolyze NAD^+ into ADP-ribose and nicotinamide (Cepeda et al., 2006).

doi:10.6342/NTU201903408

2. MATERIALS AND METHODS

Somatic cell culture

NIH/3T3 cells, HEK-293T cells, mouse embryonic fibroblast and BNL/CL2 cells were cultured in Dulbecco's Modified Eagle Medium (DMEM, 11965-084, GIBCO, U.S.A.), supplemented with 10% fetal bovine serum (FBS, 10437-028, GIBCO, U.S.A.) and 1% Penicillin/streptomycin (GIBCO, 15140). Cells were cultured in a 37°C incubator with 5% CO_2. Puromycin (A1113803, GIBCO, U.S.A.) or Hygromycin B (31282-04-9, GOLDBIO) were used to select transfected cells.

Embryonic stem cells culture

Mouse embryonic stem cells (ESCs) were cultured in DMEM with 15% FBS (040011A, Biological Industries, U.S.A. or SH3007103, Hyclone, U.S.A.), 1% Penicillin/ streptomycin (15140, GIBCO, U.S.A.), 1% GlutaMAX-I (35050-061, GIBCO, U.S.A.), 1% Non-essential amino acids (11140-050, GIBCO), 1% β-mercaptoethanol (ES-007-E, MERCK, Germany), 1% sodium pyruvate (11360-070, GIBCO) and 1000 unit/ mL mouse leukemia inhibitory factor (ESG1107, MERCK, Germany) with MEF as feeder. Transgenic-ESCs were generated by lentivirus infection.

Vector Construction

All of the construction are produced by PCR-based method. Templates were amplified by Phusion® High-Fidelity DNA Polymerase (M0530L, New England

doi:10.6342/NTU201903408

BioLabs). PCR products were clean up/ gel extraction by EasyPure PCR clean up/gel extraction kit (PG100, Bioman), then ligated by Gibson Assembly® Master Mix (E2611L, New England BioLabs). The assembly product finally were transformed into HIT competent cells JM-109 (RH-718, Bioman). The primer used were listed (Table 1). Zscan4c CDS was constructed into pSIN vector (puromycin resistant, plasmid #16578, Addgene). Parp1 CDS was brought from Sino Biological Inc. (MG50753-G, Sino Biological Inc.) then constructed into pSIN vector with replacement of puromycin resistant gene to hygromycin resistant gene. For interaction domain assay, Parp1 was truncated to 3 domains (Cepeda et al., 2006), including DNA binding domain (1-382 a.a.), auto-modification domain (383-655 a.a.) and catalytic domain (655-1014 a.a.); Zscan4 was also truncated to 3 domain (Dan et al., 2017), including SCAN domain (1-163 a.a.), Linker sequence (164-396 a.a.) and Zinc finger domain (396-506 a.a.).

Table 1. Primers for cloning and DNA sequencing.

Primers	Sequence (5'→3')	Aplications
5'-IRES	GGATCCGCATGCATCTAGGGCGG	Primer (together with 3'-EF1α) for pSIN vector cloning. Primer (together with 3'-IRES-Parp1) for *parp1* DBD domain cloning.
3'-EF1α	ACTAGTTCGAAGGATCAATTCCTCA CGACACCT	Primer (together with 5'-IRES) for pSIN vector cloning.
5'-EF-flag-Zscan4c	TGATCCTTCGAACTAGTATGGACTA CAAGGACGACGATGACAAGATGGC TTCACAGCAGGCAC	Primer (together with 3'-IRES-Zscan4c) for *zscan4c* CDS cloning.
3'-IRES-Zscan4c	GATGCATGCGGATCCTCAGTCAGA TCTGTGGTAATTCCTCAG	Primer (together with 5'-EF-flag-Zscan4c) for *zscan4c* CDS cloning.
5'-EF-HA-Parp1	TGATCCTTCGAACTAGTATGTACCC ATACGATGTTCCAGATTACGCTATG GCGGAGGCCTCGGAGAGGCTTT	Primer (together with 3'-IRES-Parp1) for *parp1* CDS cloning.

doi:10.6342/NTU201903408

3'-IRES-Parp1	GATGCATGCGGATCCTTACCACAG GGATGTCTTAAAATTGAACTTGAGT TTCAGCAGGTATTTGAGATTCACCT GAGCA	Primer (together with 3'-IRES-Zscan4c) for *parp1* CDS cloning. Primer (together with 5'-IRES) for *parp1* DBD domain cloning.
5'-Hygro	ATGAAAAAGCCTGAACTCACCGCG ACG	Primer (together with 3'-pSIN-Hygro) for hygromycin resistant gene (aminoglycoside phosphotransferase from E. coli) cloning
3'-pSIN-Hygro	GCCTATTACTATTCCTTTGCCCTCG GACGAGT	Primer (together with 5'-Hygro) for hygromycin resistant gene cloning
5'-Hygro-pSIN	AAGGAATAGTAATAGGCGGCCGCT CGAGACCTA	Primer (together with 3'-EF1α) for pSIN vector cloning (for replace with HygR).
3'-Hygro-IRES	AGTTCAGGCTTTTTCATGGAAGGTC GTCTCCTTG	Primer (together with 5'-Hygro-pSIN) for pSIN vector cloning (for replace furor with HygR).
5'-HA-P1-AMD	AGATTACGCTTCCTCTGCTCCAGC AGAC	Primer (together with 3'-P1-AMD-HA, 5'-AMD-pSIN and 3'-pSIN-AMD) for Parp1-AMD cloning. Primer (together with 3'-P1-AMD-HA) for Parp1-△DBD cloning.
3'-P1-AMD-HA	GGAGCAGAGGAAGCGTAATCTGGA ACATCG	Primer (together with 5'-HA-P1-AMD, 5'-AMD-pSIN and 3'-pSIN-AMD) for Parp1-AMD cloning. Primer (together with 5'-HA-P1-AMD) for Parp1-△DBD cloning.
5'-AMD-pSIN	AAAGAAGCTGTAAGGATCCGCATG CATCT	Primer (together with 5'-HA-P1-AMD, 3'-P1-AMD-HA and 3'-pSIN-AMD) for Parp1-AMD cloning. Primer (together with 3'-pSIN-AMD) for Parp1-△CD cloning.
3'-pSIN-AMD	GGATCCTTACAGCTTCTTTACTGCC TCTT	Primer (together with 5'-HA-P1-AMD, 3'-P1-AMD-HA and 5'-AMD-pSIN) for Parp1-AMD cloning. Primer (together with 5'-AMD-pSIN) for Parp1-△CD cloning.
5'-HA-P1-CD	AGATTACGCTACGGTGAAGCCTGG CACC	Primer (together with 3'-P1-CD-HA) for Parp1-CD cloning.

doi:10.6342/NTU201903408

3'-P1-CD-HA	CTTCACCGTAGCGTAATCTGGAACATCG	Primer (together with 5'-HA-P1-CD) for Parp1-CD cloning.
5'-SCAN	CCAGATAATTGAGGATCCGCATGCAT	Primer (together with 3’-SCAN) for Zscan4-SCAN cloning
3'-SCAN	GCGGATCCTCAATTATCTGGTGTTGGCCTTG	Primer (together with 5’-SCAN) for Zscan4-SCAN cloning
5'-LS	CGATGACAAGGAGCAGATGCCAGTAGACAC	Primer (together with 3’-LS, 5’-LS-2 and 3’-LS-2) for Zscan4-LS cloning. Primer (together with 3’-LS) for Zscan4-△SCAN cloning
3'-LS	ATCTGCTCCTTGTCATCGTCGTCCTTGTAGT	Primer (together with 5’-LS, 5’-LS-2 and 3’-LS-2) for Zscan4-LS cloning. Primer (together with 5’-LS) for Zscan4-△SCAN cloning
5'-LS-2	CTATACAAGTGAGGATCCGCATGCATCTAG	Primer (together with 5’-LS, 3’-LS and 3’-LS-2) for Zscan4-LS cloning. Primer (together with 3’-LS-2) for Zscan4-△ZF cloning
3'-LS-2	CGGATCCTCACTTGTATAGTTTGGCATCTCTACAG	Primer (together with 5’-LS, 3’-LS and 5’-LS-2) for Zscan4-LS cloning. Primer (together with 5’-LS-2) for Zscan4-△ZF cloning
5'-ZF	CGATGACAAGTGTGAAGAATGTTCTAGGATGTTC	Primer (together with 3'-ZF) for Zscan4-ZF cloning.
3'-ZF	TTCTTCACACTTGTCATCGTCGTCCTTGT	Primer (together with 5'-ZF) for Zscan4-ZF cloning.
5’-EF1α	TCAAGCCTCAGACAGTGGTTC	Primer for pSIN vector insert sequencing
3’-SP3	AGAGGAACTGCTTCCTTCACGACA	Primer for pSIN vector insert sequencing
Parp1-seq-1	AAAGCGTGTTCCACCAAC	Primer for parp1 CDS sequencing
Parp1-seq-2	GTCTAGCATCTCCACCTTG	Primer for parp1 CDS sequencing
3’-HygR-seq	AGTGGCTAAGATCTACAGC	Primer for HygR sequencing
5’-HygR-seq	TGAAGGATGCCCAGAAGG	Primer for HygR sequencing

doi:10.6342/NTU201903408

Transfection

JetPRIME transfection reagent (114-07, Polyplus) was used to transfect somatic cells or produce virus. Transfection procedures were according to protocol from manufacturers. Briefly, cells were transfected at 70-80% confluency. Suitable mount of DNA and transfection reagent were added to transfection buffer then cultured at room temperature for 10 min. Transfection pre-mix were adding into culture medium. 4 hr after co-culture, the medium was changed to fresh medium. Before infection, lentivirus was thaw on ice. $1*10^5$ cells/24 well ESCs were infected by final 2x concentration lentivirus with 8 μg/mL polybrene. Lentivirus was replaced 48h after infection. ESCs were sub-cultured and select by antibiotics 3 days after infection. Stable clones then pick up to do further experiments.

Immunofluorescent staining and florescence *in situ* hybridization (IF-FISH)

Cells were cultured on glass slide in 24-well dish. The glass slides were fix in 10% paraformaldehyde or 100% cold methanol for 15 min , and then blocked in PBS with 2.5% bovine serum albumin (A9647, Sigma) and 0.25% Triton-X100 (X100, Sigma) for 30 min at room temperature. Fixed cells then cultured with first antibody overnight at 4°C. After wash with PBS, cells cultured with second antibody for 2 hours at room temperature. Lastly, cells were staining with DAPI, and then mounted on the glass slide.

For following DNA-FISH, the protocol was according to Lazzerini Denchi E lab (Li et al., 2017) with some modification. Briefly, after IF procedures, slides were fixed in 10% formaldehyde for 2 min to prevent antibodies fade out. After wash 3 times by

doi:10.6342/NTU201903408

PBS, slides then dehydration by 70%, 95% and 100% ethanol for 5 min, consecutively. Slides were air dry for several minutes and culture up side down in hybridize solution (70% formamide, 0.5% blocking reagent, 10 mM Tris-HCl pH7.2 in deionize water, ~20 μL) with FITC-telomereC PNA probe (1:100, PANAGENE) for 10 min at 75°C (sealed in hybridize chamber and cultured in water bath). Slides then cultured in 37°C incubator for 1-3 days. After wash 2 times with wash solution (70% form amide, 10 mM Tris-HCl pH 7.2 in deionized water), slides were air dry and mounting for observation.

Immunoprecipitation

Immunoprecipitation was performed by Dynabeads protein G immunoprecipitation kit (10007D, Thermo) according to manufacturer instruction with some modification. Briefly, 50 μL of Dynabeads were used per reaction. Antibodies used for each reaction as below: 4 μg ms-IgG (550878, BD Biosciences, San Jose, CA, USA); 4 μg ms-HA (sc-7392, Santa Cruz Biotechnology, Inc., CA, USA); 2 μg Rb-IgG (550875, BD) or 2 μg Rb-FLAG (F7425, Millipore, Billerica, MA, USA). Antibody was mixed with 500 ng protein lysis in total 1 mL PBS then rotated 2 hours at 4°C. After elution, the products were analysis through western blotting.

Western blotting

Cell samples were lysised by RIPA lysis buffer (92590, Millipore) for 10 min at 4°C. After lysis, samples were centrifuged at 13,000 rpm at 4°C for 10 min then pipetted supernatant to autoclaved eppendroff tube as the protein sample. Protein

doi:10.6342/NTU201903408

samples then quantitative by diluted in protein assay dye reagent concentrate (500-0006, BioRad) and analyzed by ELISA reader (software: Perkin Elmer Wallac 1420 victor3). 30 μg protein of each sample was loading into 10% acrylamide gel for electrophoresis. Gel then transfer to 0.45 μm PVDF membrane (10600023, GE Healthcare). 5% skim milk in PBS was used to block the membrane. Following, the membrane was hybridize with first antibody overnight at 4°C. After washed 3 times by 0.1% Tween-20 in PBS, membrane hybridize with second antibody (goat-anti-mouse IgG HRP-conjugated polyclonal antibody, 31430, Thermo Fisher Scientific or goat-anti-rabbit IgG HRP-conjugated polyclonal antibody, 31460, Thermo Fisher Scientific) for 2 hr at room temperature. Finally, the membrane was detected by T-Pro LumiFast Plus Chemiluminescent Substrate Kit (JT96-K002, T-pro) and captured by GeneGnome XRQ Chemiluminescence with CCD (SynGene, Cambridge). The picture then quantitative and analysis by Image J software (Version 1.47, NIH). First antibody used in this thesis include: rabbit anti-mouse ZSCAN4 (1:1000, AB4340, Millipore), rabbit anti-mouse PARP1 (1:1000, 9542L, cell signaling), rabbit anti-FLAG probe (1:1000, F7425, Millipore) and mouse anti-HA probe (1:200, sc-7392, Santa Cruz).

3. RESULTS

3-1. Localization of ZSCAN4, PARP1 and telomere in somatic cells and ESCs

By Mass spectrum, PARP1 is predicted to be associated with ZSCAN4 previously in our lab. Therefore, I aim to validate whether PARP1 interacts with ZSCAN4. I firstly generated *Zscan4* and *Parp1* continuous expressed constructs by

doi:10.6342/NTU201903408

fused *Flag-tag* and *Ha-tag* sequence to the N-terminal of *Zscan4* open reading frame and *Parp1* open reading frame, respectively, and then inserted *Flag-Zscan4* or *Ha-Parp1* into pSIN vector with EF1α promoter. *Flag-Zscan4* and *Ha-Parp1* sequences are followed by puromycin resistant gene and hygromycin resistant gene respectively (Fig. 1A). To confirm whether the construction work or not, they were transfected into somatic cells first. Since ZSCAN4 and PARP1 are telomere-related protein, location of telomere was also detected. Because of the high-efficiency of transfection, HEK 293T cells were selected for this experiment. In HEK 293T cells, telomeres are localized at nucleolus while FLAG-ZSCAN4 and HA-PARP1 co-localized at nucleosol (Fig 1B). Consider of species-specific, mouse cell line, NIH/3T3 cells, also be tested. FLAG-ZSCAN4 and HA-PARP1 are co-localized at nucleosol while telomeres localized at nucleolus in NIH/3T3 cells (Fig. 1C).

As *Zscan4* is mainly expressed in 2-cell stage embryo and a subpopulation of ESCs (Falco et al., 2007), the localization of ZSCAN4 and PARP1 in the ESCs were also monitored. Owing to limitation of antibodies, it is difficult to detect endogenous ZSCAN4 and PARP1. As a replacement, *Flag-Zscan4* overexpression ESCs were generated. Mouse anti-FLAG antibody and rabbit anti-PARP1 antibody were used to detect exogenous ZSCAN4 and endogenous PARP1 respectively (Fig. 2). In the *Flag-Zscan4* overexpressing ESCs, FLAG-ZSCAN4 is located in the nucleosol and PARP1 is mainly located at nucleolus with part of PARP1 stays at nucleosol. Taken together, these results suggest that ZSCAN4 and PARP1 are mainly co-localized in the nucleosol.

doi:10.6342/NTU201903408

3-2. PARP1 is a ZSCAN4-interaction protein

Since co-immunoprecipitation (co-IP) is one of the best way to analysize protein-protein interaction, the aim is to validate whether PARP1 interacts with ZSCAN4 by co-IP. Endogenous co-immunoprecipitation (co-IP) is firstly be done. However, due to only 1-5% of cells expressed ZSCAN4, I failed to get the result from endogenous co-IP (data not shown). Alternatively, *Flag-Zscan4* and *Ha-Parp1* were transfected into HEK-293T , and then cells were harvested for co-IP. To avoid false-positive co-IP result, the protein lysate was immunoprecipitated by either FLAG antibody or HA antibody, respectively. Mouse IgG isotype or rabbit IgG isotype are controls for antibodies to prevent non-specific precipitation result. By immunoprecipitated with HA antibody, FLAG was detected at 72 kDa, the same molecular mass as ZSCAN4 (Fig. 3A). Moreover, by immunoprecipitated with FLAG antibody, HA signal can also be detected at 106 kDa, same as PARP1 (Fig. 3B). In summary, mass spectrum prediction was confirmed that PARP1 is a ZCAN4-interaction protein.

3-3. ZSCAN4 interacted with PARP1 through SCAN domain and Zinc finger domain

Further, the interaction domain of ZSCAN4 with PARP1 was investigated. According to Dan et al., 2017, *Zscan4* was truncated into three domains, including SCAN domain (SCAN, 1-163 a.a.), linker sequence (LS, 164-396 a.a.) and zinc finger domain (ZF, 397-506 a.a., Fig. 4A). Domains were fused with *flag tag* to be detected. To confirm constructions are successful, they are delivered into HEK 293T cells with *Ha-Parp1* followed by immunostaining. The result shows that all the construction can

doi:10.6342/NTU201903408

be co-expressed with *Ha-Parp1* successfully. Among groups, only full length ZSCAN4 located at nucleus while single domains located at cytosol, suggesting that the truncated Zscan4 has different expression location (Fig. 4B).

Next, full length of *Flag-Zscan4* and 3 different truncated *Flag-Zscan4* were co-transfected with *Ha-Parp1* into HEK 293T cells respectively for co-IP. Within groups, full length *Flag-Zscan4* and full length *Ha-Parp1* group serves as positive control. Precipitated by HA antibody, SCAN and ZF have been detected at ~20 and ~11 kDa, separately (Fig. 4C). According to sequence, the prediction size of SCAN and ZF is 19.64 kDa and 14.37 kDa respectively, it is reasonable to believe the signal is come from the target. By FLAG antibody, PARP1's signal also be detected in SCAN and ZF groups (Fig. 4D). Collectively, the result indicated that ZSCAN4 interacts with PARP1 though SCAN domain and Zinc finger domain.

3-4. PARP1 interacted with ZSCAN4 through DNA binding domain and automodification domain

On the other hand, interaction domains of PARP1 are also investigated. PARP1 was truncated into 3 domains, including DNA binding domain (DBD, 1-382 a.a.), automodification domain (AMD, 383-655 a.a.) and catalytic domain (CD, 656-1014 a.a., Fig. 5A). Constructions were fused with *Ha tag* to be detectable (Cepeda *et al*., 2006). The construction was then delivered into HEK 293T with full length *Flag-Zscan4* for immunostaining. All the constructions can be co-expressed with *Flag-Zscan4* successfully (Fig. 5B). Interestingly, full length PARP1 and DBD localized at nucleus while automodification domain and CD were detected at cytosol. This result

doi:10.6342/NTU201903408

indicated that the nucleus localization signal of PARP1 is in the DNA binding domain, which is consistent with the previously published paper (Cepeda *et al*., 2006).

Next, the same construct set was performed co-IP. By HA antibody, ZSCAN4's signals were detected in DBD and AMD groups, demonstrated that PARP1 interacts with ZSCAN4 through DBD and AMD (Fig. 5C). However, applied co-IP by FLAG antibody, only DBD signal be detected at ~48 kDa, which the prediction size is 44 kDa (Fig. 5D). These result imply that PARP1 may interact with ZSCAN4 majorly by DBD with AMD in the minor.

3-5. SCAN domain of ZSCAN4 interacts with both DBD and AMD of PARP1 while ZF of ZSCAN4 binding with only AMD of PARP1

To further clarify the exactly interaction domain of both ZSCAN4 and PARP1, co-IP of single domain were performed. SCAN domain or ZF domain was co-transfected with full length Parp1, DBD or AMD domain. Full length Zscan4 and Parp1 group was served as positive control. In SCAN domain part, by HA antibody, SCAN domain has been interacted with both DBD and AMD domain (Fig. 6A). However, precipitated by FLAG antibody, only DB signal can be detected (Fig. 6B). The result indicated that SCAN domain of ZSCAN4 may majorly interact with DB domain of PARP1 with AM domain in the minor. In the part of ZF domain, immunoprecipitation performed by both HA and FLAG domain indicated that ZF domain of ZSCAN4 interact with only AM domain of PARP1 (Fig. 6C-D).

doi:10.6342/NTU201903408

In summary, the interaction domain of PARP1 and ZSCAN4 is discovered in this chapter. SCAN domain of ZSCAN4 interacts with both DB domain and AM domain of PARP1, while ZF domain interacts with only AM domain (Fig. 7).

doi:10.6342/NTU201903408

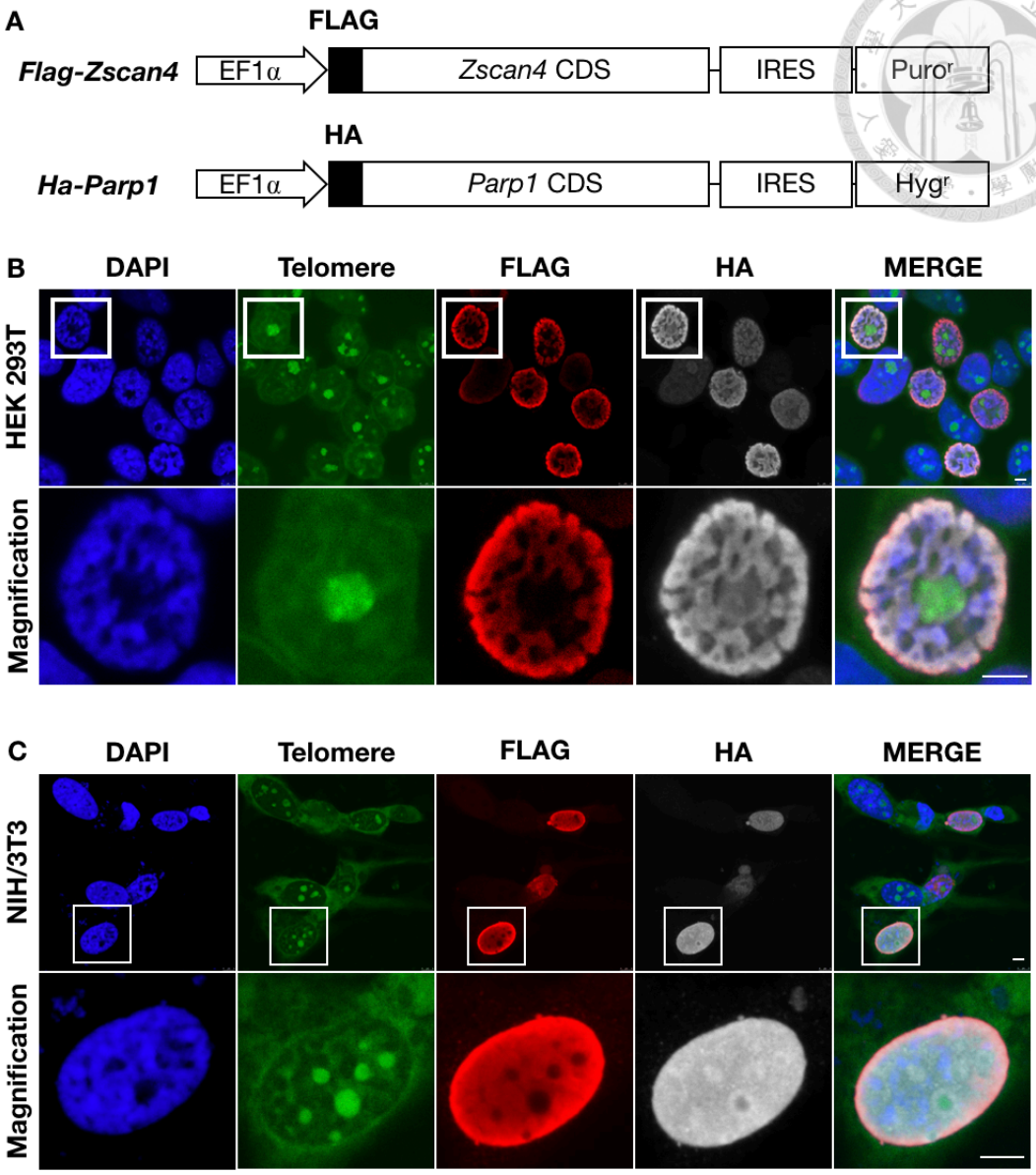

Figure 1. Localization of exogenous ZSCAN4, PARP1 and telomere sequence in somatic cells.

(A) partial plasmid map of constructions. (B) IF-FISH of *flag-zscan4* and *ha-parp1* co-transfected HEK-293T cells. (C) IF-FISH of *flag-zscan4* and *ha-parp1* co-transfected NIH/3T3 cells. In somatic cells, exogenous ZSCAN4 and PARP1 co-localize at nucleosol. Scale bars: 5 μm.

doi:10.6342/NTU201903408

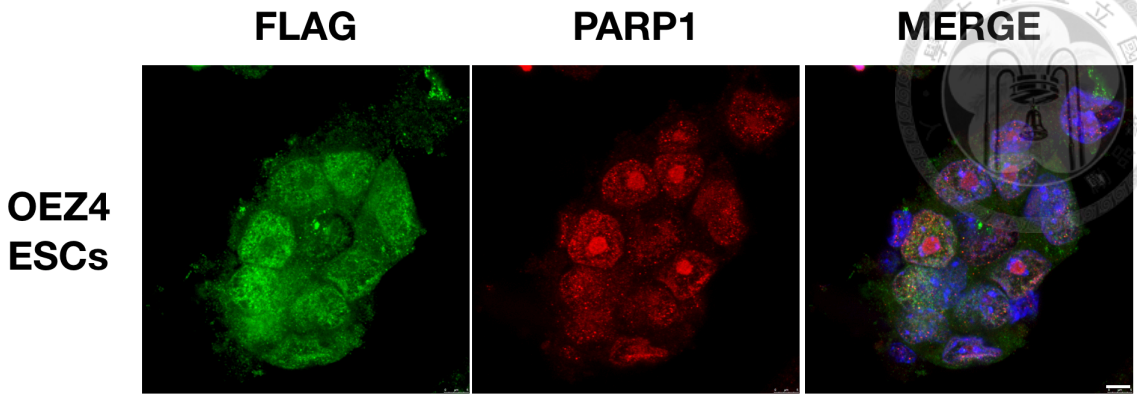

Figure 2. Localization of exogenous ZSCAN4 and PARP1 in stable *Flag-Zscan4* over expression ESCs.

Flag-Zscan4 is infected into ESCs by lentivirus. Stable clone was picked up after selected by puromycin. Exogenous ZSCAN4 and endogenous PARP1 co-localize at nucleosol. Scale bars: 5 μm.

doi:10.6342/NTU201903408

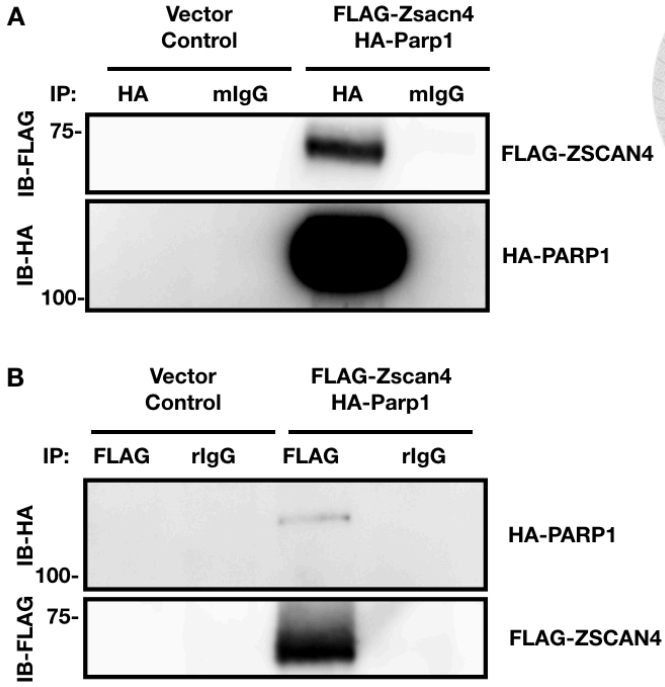

Figure 3. ZSCAN4 and PARP1 interact with each other.

Plasmids are transfected into HEK 293T cells, and then harvest 24 hr after transfection. 500 μg of protein lysate per reaction is immunoprecipitated by either (A) HA antibody or (B)FLAG antibody. The result confirms PARP1 as a ZSCAN4-associated protein.

doi:10.6342/NTU201903408

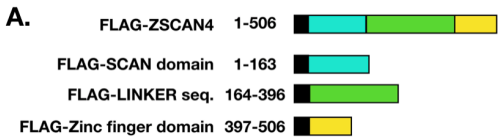

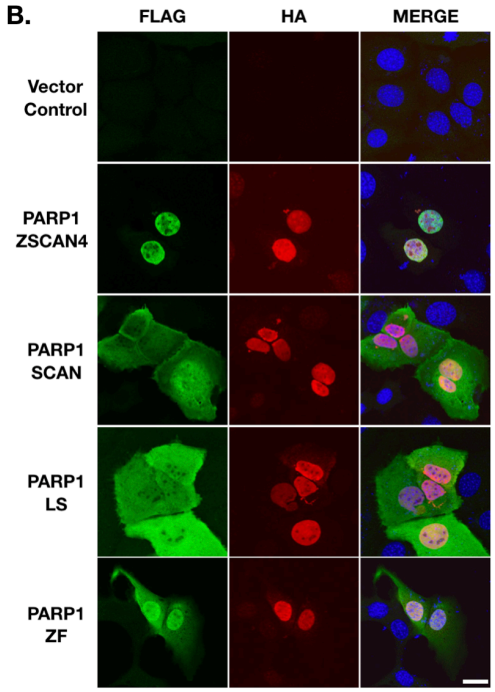

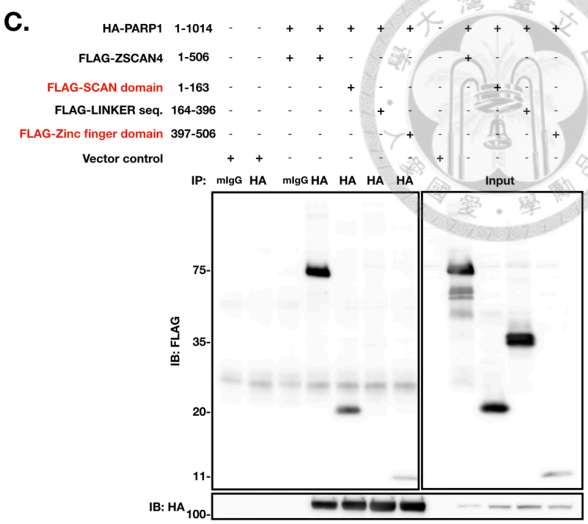

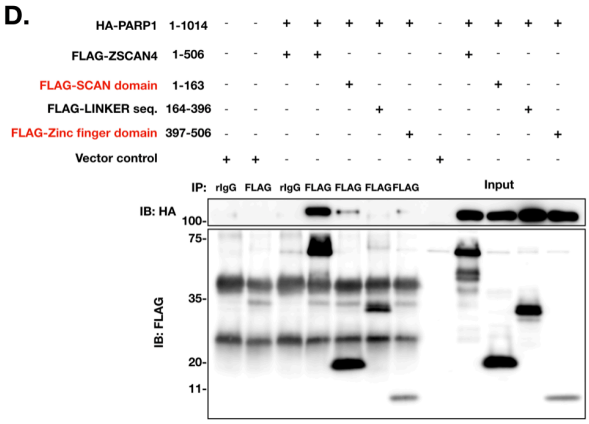

doi:10.6342/NTU201903408

Figure 4. ZSCAN4 associated with PARP1 through SCAN domain and Zinc finger domain.

(A) Schematic diagram of different *Zscan4* domains. The number represents amino acid sequence. Black bar: flag tag (FLAG). Cycan bar: SCAN domain (SCAN). Green bar: linker sequence (LS). Yellow bar: Zinc finger domain (ZF). (B) Immunostaining of mouse BNL CL2 cells transfected with different domain of *Flag-Zscan4* and *Ha-Parp1* by FLAG and HA antibodys. Scale bar: 15 μm. (C-D) Immuniprecipitation of full length PARP1 and truncated ZSCAN4 by (C) HA antibody (sc-7392, Santa cruz) and (D) FLAG antibody (F7425, SIGMA). 500 μg of protein lysates were used for each reaction. Input control were 10 μg of protein lysate.

doi:10.6342/NTU201903408

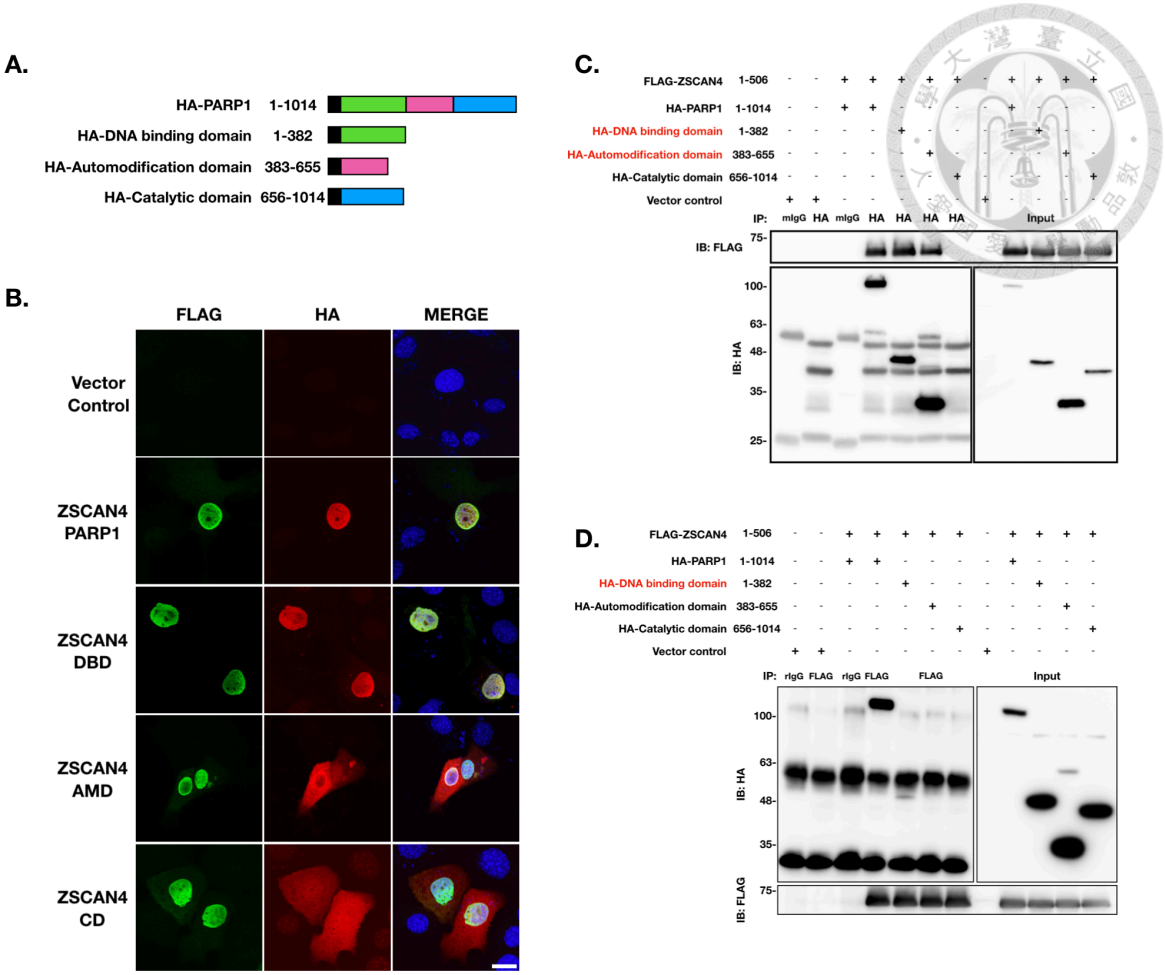

Figure 5. PARP1 associates with ZSCAN4 through DNA binding domain and auto-modification domain.

(A) Schematic diagram of *Parp1* domains. The number represents amino acid sequence. Black bar: HA tag (HA). Green bar: DNA binding domain (DBD). Pink bar: automodification domain (AMD). Blue bar: catalytic domain (CD). (B) Immunostaining of mouse BNL CL2 cells transfected with different domain of *Ha-Parp1* and *Flag-Zscan4* by HA and FLAG antibody. Scale bar: 15 μm. (C-D) Immuniprecipitation of full length ZSCAN4 and truncated PARP1 by (C) HA antibody (sc-7392, Santa cruz) and (D) FLAG antibody (F7425, SIGMA). 500 μg of protein lysates were used for each reaction. Input control were 10 μg of protein lysate.

doi:10.6342/NTU201903408

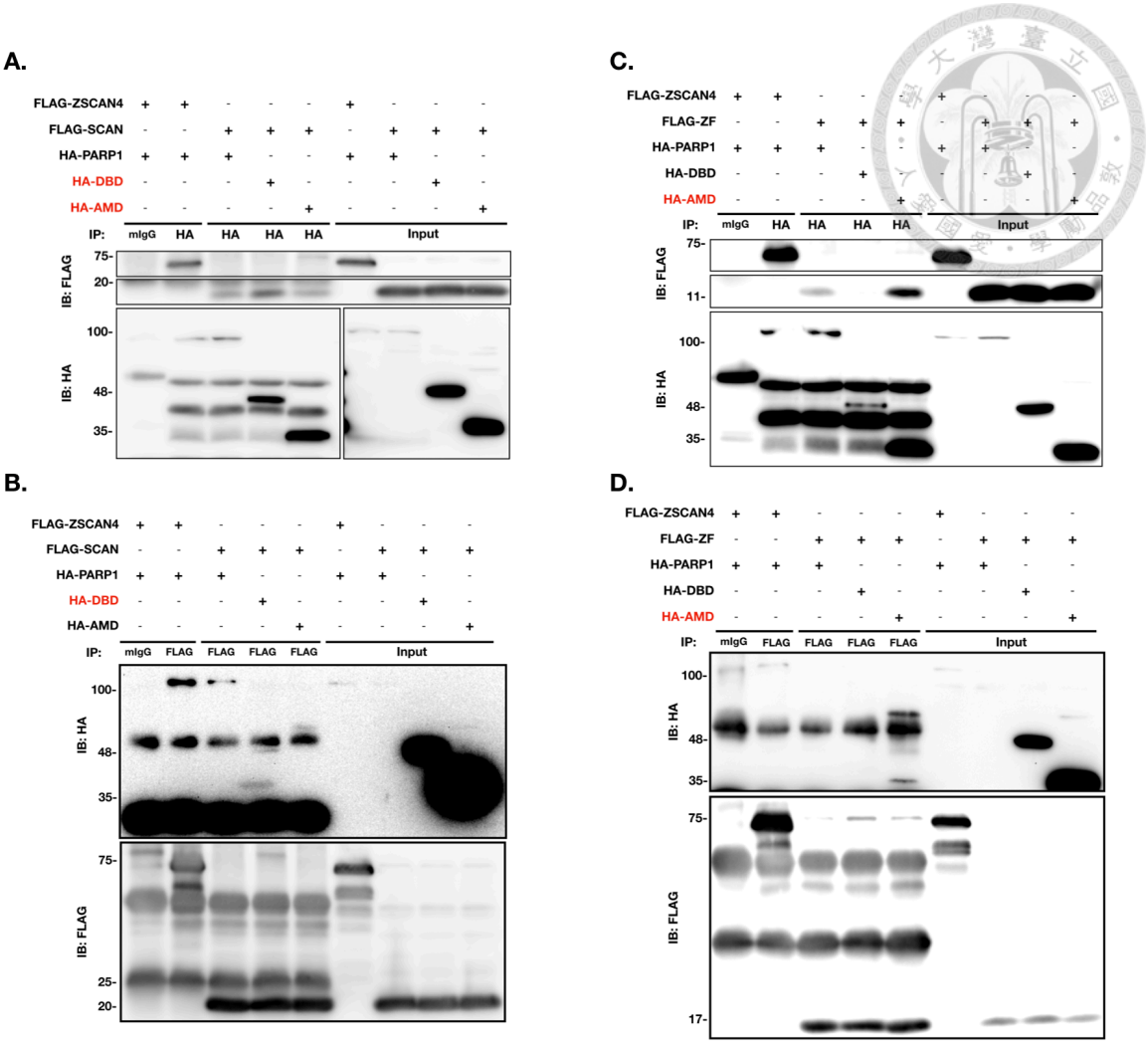

Figure 6. SCAN domain of ZSCAN4 interacts with both DBD and AMD of PARP1 while ZF domain of ZSCAN4 binding with AMD

(A-B) Immuniprecipitation of SCAN of Zscan4 and DBD or AMD of PARP1 by (A) HA antibody (sc-7392, Santa cruz) and (B) FLAG antibody (F7425, SIGMA). (C-D) Immuniprecipitation of ZF of Zscan4 and DBD or AMD of PARP1 by (A) HA antibody (sc-7392, Santa cruz) and (B) FLAG antibody (F7425, SIGMA). 500 μg of protein lysate is used for each reaction. Input control is 10 μg of protein lysate.

doi:10.6342/NTU201903408

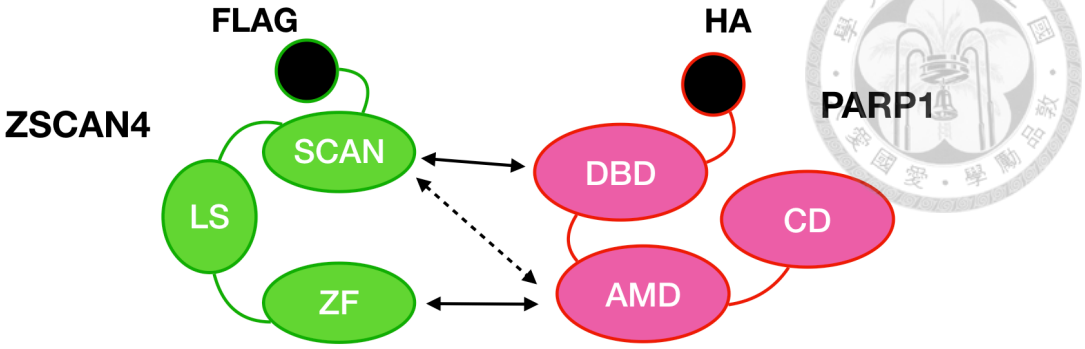

Figure 7. Schematic diagram of interaction domains of ZSCAN4 and PARP1.

SCAN domain of ZSCAN4 interests with both DBD and AMD of PARP1, while ZF domain mainly interacts with AMD of PARP1. Solid lines mean the interaction are major. Dotted line means the interaction is minor.

doi:10.6342/NTU201903408

4. DISCUSSION

ZSCAN4 has been shown to interact with several proteins (Dan et al., 2013; Dan et al., 2017). However, how *Zscan4* affects telomere length, potency and epigenetic is still unclear. Therefore, in this thesis I tried to understand more about mechanisms of ZSCAN4 participate in telomere length regulation through investigating the proteins associated with ZSCAN4.

Ectopically expressed ZSCAN4 and PARP1 localized at nucleoplasm while telomeres localized in nucleolus, imply that ZSCAN4 may not directly affect telomere length but elongate telomere length through transcription factor mechanism (Nishiyama et al., 2009). On the other hand, PARP1 has been reported to bind to TRF2, a subunit of shelterin (Gomez et al., 2006). Yet, in the cells I investigated, PARP1 majorly localized at nucleoplasm but not localized with telomere in nucleolus at G1/0 phase, based on existence of nucleolus. These results combine with previous paper indicate that PARP1 may only bind with telomere in some specific cell events, e.g. H_2O_2 treatment (Gomez et al., 2006).

Nuclear localization signal (NLS) is the short sequence take the protein into the nucleus. Since ZSCAN4 located in nucleus, I expected to discover NLS through truncated *Zscan4 (Dan et al., 2017)*. However, although ZF domain majorly located in the nucleus, I still detected signal in cytoplasm. The result failed to discover the clear NLS in *Zscan4.* Since the online sequence predicted the NLS of *Zscan4* is at 382-408 a.a.*,* it may due to destroy of NLS in truncated form of *Zscan4* (Kosugi et al., 2009). On the other hand, in truncated PARP1, I investigated only DBD localized in nucleus while AMD and CD are detected at cytoplasm. The result shows similar truth as previous papers that NLS of PARP1 is at DNA binding domain (Cepeda et al., 2006).

doi:10.6342/NTU201903408

To validate protein-protein interactions, the most direct way is to immunoprecipitate endogenous protein. Unfortunately, due to limitation of ZSCAN4 expression level, which only 1-5% of ESCs expressed ZSCAN4, I failed to perform endogenous Immunoprecipitation (data not showed, Zalzman et al., 2010). Alternatively, by exogenously expressed *Flag-Zscan4* and *Ha-Parp1*, serial immunoprecipitations have been applied. The Mass spectrum data has been confirmed that PARP1 is a ZSCAN4 associated protein.

Numerous conserved protein domains share the similar function. Zscan4 has been defined as 3 regions: SCAN domain, linker sequence and Zinc finger domain. Here, I found that ZSCAN4 binds with PARP1 through SCAN domain and Zinc finger domain. Both SCAN domain and Zinc finger domain shows ability to interact with other proteins in previous papers (Williams et al., 1999; Edelstein and Collins, 2005; Vilas et al., 2018). Further, PARP1 interacts with Zinc finger domain which functions as DNA binding domain, indicating that PARP1 may affect ZSCAN4's DNA binding ability. On the other hands, PARP1 interacts with ZSCAN4 via DNA binding domain and automodification domain. Automodification domain is the site accepted ADP-ribose and also allowed PARP1 to form homo-dimer (Cepeda et al., 2006). Since PARP1 activates after binding to DNA, ZSCAN4 may also affect PARP1's enzyme activity, even ZSCAN4 do not directly interact with catalytic domain.

The limitation of this experiment is that the protein is exogenously expressed. Instead of normal physiological concentration of proteins, the concentration of proteins are dramatically higher, which may cause false positive. Second, due to the transfected efficiency, HEK 293T cells were chose as host, which can not exclude the possibility

doi:10.6342/NTU201903408

that the protein structures are different then in mouse. However, due to each of domain set is performed both FLAG and HA antibody, the data must have certain credibility.

Collectively, in this chapter, I not only validated previous Mass spectrum prediction that PARP1 interacts with ZSCAN4 but also discovered their interaction domains . To investigate the meaning of their interaction, further experiments based on the interaction domain will be necessary.

doi:10.6342/NTU201903408

CHAPTER III:

FUNCTION OF PARP1 INTERACTS WITH ZSCAN4 IN TELOMERE HOMEOSTASIS

doi:10.6342/NTU201903408

1. BACKGROUND

The most famous function of *Zscan4* is to elongate telomere through ALT pathway, which is a telomerase independent pathway (Zalzman et al., 2010; Dan et al., 2017). It has been reported that the *Zscan4* expressed ESCs show repression of protein synthesis (Hung et al., 2013). Moreover, *Zscan4* is activated by short telomere length and the *Zscan4* expressed ESCs shows higher percentage of cell at G2/M phase (Nakai-Futatsugi and Niwa, 2016).

On the other hand, *Parp1* is well-known for sensing DNA damage. Previous studies indicated that Parp1 also involved in telomere regulation. PARP1 co-localized with TRF2, a telomere binding protein, after hydroperoxide treatment (Gomez et al., 2006). Parp1 deficiency mice has shorted telomere and accelerated aging (d'Adda di Fagagna et al., 1999). PARP inhibition has been used as a tumor therapy for a long time (Cepeda et al., 2006). 3-aminobenzamide is the first generation of PARP inhibitor which competed with NAD^+, the substrate of PARP1, to inhibit PARPs enzyme activity (Cepeda et al., 2006).

Regulation of telomere length is a complicated pathway with a lots of genes involved. In this study, I picked up several telomere-related genes to test, which can be classified into 2 subsets: repression of Zscan4 or homologous recombination (Rif1, Atrx, Suv39h2 and Dnmt3b) and activation of Zscan4 or HR (Rtel1, Telo2 and Tbx3). *Rif1* has been reported to inhibit *Zscan4* promoter activity in mouse ESCs. Further, *Rif1* maintain H3K9me3 at sub-telomeric region which has the *Zscan4* sequence on it (Dan et al., 2014). *Atrx*, is a gene mediated H3K9me3 with *Suv39h1* and absent in ALT cells. *Atrx* is also found to be inhibiting ALT pathway (Tardat and Dejardin, 2018). *Suv39h2* and *Dnmt3b* are responsible for establish H3K9me and DNA methylation, respectively

doi:10.6342/NTU201903408

(Dan et al., 2017). It have been reported that *Rtel1* prevents gene instability and increases T-SCE rate (Zalzman et al., 2010). *Telo2* is a gene involving in DNA damage response and regulating PI3K pathway (Takai et al., 2007). *Zscan4* has been reported to be regulated by PI3K pathway (Storm et al., 2014). Lastly, *Tbx3* has been shown to inhibit DNMT3B binding to *Zscan4* promoter in mouse ESCs and further derepressed *Zscan4* expression level (Dan et al., 2013).

In the chapter II, I have validated PARP1 as a ZSCAN4-associated protein. Since Zscan4 and Parp1 are both be reported as a telomere-related gene, the effect of their interaction on telomere length regulation will be investigated in this chapter.

doi:10.6342/NTU201903408

2. MATERIALS AND METHODS

Somatic cell Culture

NIH/3T3 cells and MEF were cultured in Dulbecco's Modified Eagle Medium (DMEM, 11965-084, GIBCO, U.S.A.), suppling with 10% fetal bovine serum (FBS, 10437-028, GIBCO, U.S.A.) and 1% Penicillin/streptomycin (GIBCO, 15140). Cells were cultured in a 37°C incubator with 5% CO_2. Puromycin (A1113803, GIBCO, U.S.A.) and/or Hygromycin B (31282-04-9, GOLDBIO) were used to select transfected cells.

Embryonic stem cells culture

Mouse embryonic stem cells (ESCs) were cultured in DMEM with 15% FBS (040011A, Biological Industries, U.S.A. or SH3007103, Hyclone, U.S.A.), 1% Penicillin/streptomycin (15140, GIBCO, U.S.A.), 1% GlutaMAX-I (35050-061, GIBCO, U.S.A.), 1% Non-essential amino acids (11140-050, GIBCO), 1% β-mercaptoethanol (ES-007-E, MERCK, Germany), 1% sodium pyruvate (11360-070, GIBCO) and 1000 unit/ mL mouse leukemia inhibitory factor (ESG1107, MERCK, Germany) with MEF as feeder. Transgenic-ESCs were generated by lentivirus infection. For PARP1 inhibitor experiment, stock of 3-aminobenzamide (3-AB, A0788, Sigma) was dissolved in DMSO while 0.1% DMSO serves as control. Parp1 short hairpin RNAs (shRNA) are provided by National RNAi Core Facility at Academia Sinica in Taiwan. shRNA was infected into ESCs by lentivirus. LacZ shRNA serves as control. The Parp1

doi:10.6342/NTU201903408

shRNA target sequences are: GCAAGAAATGCAGCGAGAGTA (Parp1 shRNA1) and GCCCTTGGAAACATGTATGAA (Parp1 shRNA2).

Terc$^{+/-}$ nuclear transfer ESCs were previously generated by Dr. Sung (Sung et al., 2014) while the donor cell was provided by Jackson's lab. The *Terc*$^{+/-}$ donor cell was generated by replaced *Terc* with neomycin resistance gene. Followed, the trans-gene ESCs were used to produce *Terc*$^{+/-}$ mice by blastocyst injection. (Blasco et al., 1997) Genotyping of Terc$^{+/-}$ ntESCs was done by PCR with primers as listed (Table. 2). The PCR process is: 95°C 30 sec; 62°C 30 sec; 72°C 30 sec for 35 cycles. The PCR product then detected by agarose electrophoresis. For *Terc*, the the signal after agarose electrophoresis can be detected at 150 b.p. while the band at 280 b.p. represents neomycin resistant gene.

Table 2. Primers for Terc genotyping.

Primers	Sequence (5'→3')
oIMR1912	CTCGGCACCTAACCCTGAT
oIMR1913	CGCTGACGTTTGTTTTTGAG
oIMR6916	CTTGGGTGGAGAGGCTATTC
oIMR6917	AGGTGAGATGACAGGAGATC

Vector Construction

All of the construction are produce by PCR-based method. Templates were amplified by Phusion® High-Fidelity DNA Polymerase (M0530L, New England BioLabs). PCR products were clean up/ gel extraction by EasyPure PCR clean up/gel extraction kit (PG100, Bioman), then ligated by Gibson Assembly® Master Mix

doi:10.6342/NTU201903408

(E2611L, New England BioLabs). The assembly product finally be transformed into HIT competent cell JM-109 (RH-718, Bioman). The primer used were listed (Table 1). *Zscan4c* CDS was constructed into pSIN vector (puromycin resistant, plasmid #16578, Addgene). *Parp1* CDS was purchased from Sino Biological Inc. (MG50753-G, Sino Biological Inc.), and then constructed into pSIN vector with replacing puromycin resistant gene to hygromycin resistant gene.

Production of lentivirus and infection

Platinum-E cell line (RV-101, Cell Biolabs) was used to package lentivirus. Interested gene was co-transfected with psPAX2 (plasmid #12260, Addgene) and pMD2.G (plasmid #12259, Addgene). Lentivirus were then harvested 48h and 72h after transfection. Toolsilent lentiPrecipitating reagent (VCT-KA00-100, Biotools) was used to concentrate lentivirus to 100x. Lentivirus was stocked at -80°C. Before infection, lentivirus was thawed on ice. $1*10^5$ cells/24 well ESCs were infected by final 2x lentivirus with 8 μg/mL polybrene. Lentivirus was removed 48h after infection. ESCs were sub-cultured and select by antibiotics 3 days after infection. Stable clones then pick up to do further experiments.

Transfection

JetPRIME transfection reagent (114-07, Polyplus) was used to transfect somatic cells or produce virus. Transfection procedures were according to protocol from manufacturers. Briefly, cells were transfected at 70-80% confluency. Suitable mount of

doi:10.6342/NTU201903408

DNA and transfection reagent were added to transfection buffer, and then cultured at room temperature for 10 min. Transfection pre-mix was added into culture medium. 4 hr after co-culture, the medium was changed by fresh medium. Cells are harvested 24-48 hr after transfection.

Western blotting

Cell samples were lysised by RIPA lysis buffer (92590, Millipore) for 10 min at 4°C. After lysis, samples were centrifuged at 13,000 rpm at 4°C for 10 min then pipetted supernatant to autoclaved eppendroff tube as the protein sample. Protein samples then quantified by diluted in protein assay dye reagent concentrate (500-0006, BioRad) and analyzed by ELISA reader (software: Perkin Elmer Wallac 1420 victor3). 30 μg protein of each sample was loaded into 10% acrylamide gel for electrophoresis. Gel then transfer to 0.45 μm PVDF membrane (10600023, GE Healthcare). 5% skim milk in PBS was used to block the membrane. Following, the membrane was hybridized with first antibody overnight at 4°C. After washed 3 times by 0.1% Tween-20 in PBS, membrane was hybridized with second antibody (goat-anti-mouse IgG HRP-conjugated polyclonal antibody, 31430, Thermo Fisher Scientific or goat-anti-rabbit IgG HRP-conjugated polyclonal antibody, 31460, Thermo Fisher Scientific) for 2 hr at room temperature. Finally, the membrane was detected by T-Pro LumiFast Plus Chemiluminescent Substrate Kit (JT96-K002, T-pro) and captured by GeneGnome XRQ Chemiluminescence with CCD (SynGene, Cambridge). The picture then quantified and analyzed by Image J software (Version 1.47, NIH). First antibody used in this thesis include: rabbit anti-mouse ZSCAN4 (1:1000, AB4340, Millipore), rabbit anti

doi:10.6342/NTU201903408

mouse PARP1 (1:1000, 9542L, cell signaling), rabbit anti-FLAG (1:1000, F7425, Millipore) and mouse anti-HA (1:200, sc-7392, Santa Cruz).

Immunofluorescent staining and florescence *in situ* hybridization

Cells were cultured on glass slide in 24 wells dish. The glass slides were fix in 10% paraformaldehyde or 100% cold methanol for 15 min then blocked in PBS with 2.5% bovine serum albumin (A9647, Sigma) and 0.25% Triton-X100 (X100, Sigma) for 30 min at room temperature. Fixed cells were then cultured with first antibody overnight at 4°C. After washing with PBS, cells cultured with second antibody for 2 hours at room temperature. Lastly, cells were stained with DAPI then mounting on the glass slide. laser-scanning confocal microscope (Leica TCS SP5 II confocal microscope) was used to acquire images.

Telomere/single copy gene ratio (T/S ratio)

Genomic DNA was extracted by gSYNC DNA extraction kit (GS100, Geneaid, New Taipei City, Taiwan). 20 ng of sample genomic DNA was mix with primers for telomere or single copy gene (*36b4*), respectively. The sample was then mixed with Heiff qPCR SYBR Green master mix (11203ES03, YEASEN Shanghai, China) and performs quantitative polymerase chain reaction (the Roche Light Cycler, LC480, Roche Applied Science, Mannhein, Germany). Genomic DNA of vector control group was used to prepare standard curve for absolute quantification in every trial. Primers were listed as below:

doi:10.6342/NTU201903408

Table 3. Primers for T/S ratio.

Primers	Sequence (5'→3')
5'-telomere	CGGTTTGTTTGGGTTTGGGTTTGGGTTTGGGTTTGGGTT
3'-telomere	GGCTTGCCTTACCCTTACCCTTACCCTTACCCTTACCCT
5'-36b4	ACTGGTCTAGGACCCGAGAAG
3'-36b4	TCAATGGTGCCTCTGGAGATT

Quantitative Real-Time Polymerase Chain Reaction (qRT-PCR)

Total RNA was extracted by Azol (Azol.200, ArrowTEC), and then removed DNA by RQ1 RNase-free DNase (M6101, Promega). 20 ng of cDNA was used per reaction. cDNA was mixed with Heiff qPCR SYBR Green master mix (11203ES03, YEASEN Shanghai, China) and performs quantitative polymerase chain reaction (the Roche Light Cycler, LC480, Roche Applied Science, Mannhein, Germany). Primers for qRT-PCR were listed in Table 4.

Table 4. Primers for qRT-PCR.

Primers	Sequence (5'→3')
5'-Gapdh	TGGCC TTCCG TGTTC CTA C
3'-Gapdh	GAGTT GCTGT TGAAG TCGCA
5'-Parp1	CAAGTCCAACAGGAGCATGTGCAA
3'-Parp1	CGCATCTGGCCCTTCTCTATCTTC
5'-Zscan4	AAATGCCTTATGTCTGTTCCCTATG
3'-Zscan4	TGTGATAATTCCTCAGGTGACGAT
5'-Terc	GGGTT CTGGT CTTTT

doi:10.6342/NTU201903408

3’-Terc	CTGCA GGTCT GGACT TTCCT
5’-Tert	TGAAA GTAGA GGATT GCCAC TG
3’-Tert	AGCCA GAACA GGAAC GTAGC
5’-Rif1	CAAG GATGT TGAGA CTGAG C
3’-Rif1	TAGAG GCACT GGCAA GTATG TC
5’-Suv39h2	ATTCA GCTGG AGCCT GATTC CTCA
3’-Suv39h2	TACAT GGTTC CAGCC TCTGC TCAA
5’-Tbx3	CGGAA GTCCC ATTAT CCTCA ACCT
3’-Tbx3	GAACT AATGG TCCAA CAGGC ACAC
5’-Dnmt3b	GCACA ACCAA TGACT CTGCT GCTT
3’-Dnmt3b	AGGAC AAACA GCGGT CTTCC AGAT
5’-Telo2	TTGTG GTTAC CCGCA AGC
3’-Telo2	CAAGT ACCCC AACAG GCTCT
5’-Terf2	TCAGC TGCTT CAAGT ACAAT GAG
3’-Terf2	GGTTC TGAGG CTGTC TGCTT
5’-Rtel1	CAAGC AGCAG TTTGA GGACA
3’-Rtel1	CAGAC AAGGT CAGTT TAGAC TCCA
5’-Atrx	TTGCC AAAAG GTACA GTGAT TGT
3’-Atrx	CGCGT TTTAT GAGAT TGTCA GC

doi:10.6342/NTU201903408

3. RESULTS

3-1. *Zscan4* over-expressed ESCs shows slower proliferative rate and longer telomere length

ZSCAN4 is famous for the ability to increase telomeres length through ALT of telomere pathway. Thus, whether PARP1 involves in ZSCAN4's function on telomere elongation is needed to be investigated. Firstly, *Flag-Zscan4* overexpression ESCs (OEZ4 ESCs) have been generated and the expression of endogenous ZSCAN4 and FLAG were confirm by double staining. The result showed that ZSCAN4 were co-localized with FLAG (Fig. 8A). By western blot, protein expression level of ZSCAN4 and PARP1 were further detected (Fig. 8B-D). The result shows that PARP1 does not have trending change according to ZSCAN4 overexpression. Additionally, OEZ4 ESCs showed significantly slower proliferation rate and longer cell doubling time compared to vector control (Fig. 8E, F). These result may due to telomere elongation by *Zscan4* directly or indirectly decrease cell cycle. Moreover, elongation of telomere has been detected by T/S ratio in OEZ4 ESCs which is consistent with previously published paper (Dan et al., 2017) (Fig. 8G). However, Overexpression of *Zscan4* in somatic cell line, NIH/3T3 cells, do not show change of proliferation rate and telomere length, suggests that function of *Zscan4* may be ESCs specific due to dramatical gene profile difference (Fig 9A-C).

doi:10.6342/NTU201903408

3-2. Inhibition of PARP1 affects telomere homeostasis

In following experiments, OEZ4 ESCs were treated with 3-aminobenzamide (3-AB), an inhibitor for PARPs activity, to test whether PARP1 plays a role in ZSCAN4 dependent telomeres elongation. PARP1 has the ability to transfer the ADP-ribose from NAD^+ to the acceptor protein, and then produced nicotinamide as a side product. 3-AB is an analog of NAD^+ which can competitively block the enzyme activity. The concentrations of 3-AB was according to previous papers (Gao et al., 2009; Okashita et al., 2016). Duration was decided in the light of lab's previous tests on different small molecular drugs which affect the telomere length (data not shown). After three passages of treatment of 3-AB with different concentration in OEZ4 ESCs, the telomere shortened to the equivalent length to vector control, which indicated that the elongation of telomeres depends on enzyme activity of PARP1 in ZSCAN4 continuously expressing ESCs (Fig. 10). Surprisingly, telomere length slightly elongated in vector control group (i.e. wild-type) after 3 passages of 3-AB treatment, suggesting that PARP1 may also have the ability to inhibit telomere lengthening in ESCs (Fig. 10). Our data suggest that PARP1 not only involves in ZSCAN4 induced telomere elongation but may also play dual rules in telomere homeostasis.

3-3. Knockdown of Parp1 leads to Zscan4 derepression and telomere elongation

Since telomeres have been found elongated in vector control (i.e. wild-type) of 3-AB experiment (Fig. 10), I am curious about whether this elongation effect is directly caused by ZSCAN4. Hence, I further generated Parp1 knockdown ESCs clones by introducing 2 different short hairpin RNAs (shRNA) to further confirm our inhibitor

doi:10.6342/NTU201903408

result. After *Parp1* knockdown ESCs clones were generated, qRT-PCR was firstly used to validate Parp1 knockdown efficiency. *Parp1* mRNA expression level shows average 70%~80% knockdown efficiency between clones compared with *shlacZ* control (Fig 11A). Further, protein level of PARP1 was measured by western blot. PARP1 also shows >70% knockdown efficiency compared with *shlacZ* control (Fig 12A-B). The quantitative analysis validated the successful *Parp1* knockdown ESCs clones. Excitingly, Zscan4 expression level shows significantly enhance both in transcriptional and translational level (Fig. 11B, Fig. 12C). The result demonstrated that PARP1 expression level decreased accomplished by higher expression level of ZSCAN4, implying that ZSCAN4 could be inhibited by PARP1. Furthermore, telomeres elongated significantly after knockdown of Parp1 for 10 passages, compared to shlacZ control (Fig. 12D). Additionally, the mRNA level of telomerase components, *Terc* and *Tert*, do not show trend change after knockdown of *Parp1* (Fig. 11C-D). Hence, the significance change of *Terc* and *Tert* were contributed to clone specificity. Further, by qRT-PCR, I tried to investigate the mechanisms of how *Parp1* affects expression level of *Zscan4*. According to previous papers, several chromatin remodeling and telomere-related genes have been tested (Huang et al., 2011; Dan et al., 2013; Dan et al., 2014). After knockdown of *Parp1*, increased expression level of *Tbx3* be detected, which has been reported reduced DNMT3B binding to sub-telomeric region and derepressed of the gene at sub-telomere, like *Zscan4* (Dan et al., 2013). However, *Dnmt3b*, the target of *TBX3*, does not show decreased after knockdown of Parp1 (Fig. 11H, L). On the other hand, *Suv39h2*, the gene responsible for H3K9me3, do not shows change of expression level either (Fig. 11G). Surprisingly, *Rif1*, *Rtel1* and *Atrx*, which are involved in prevented genome instability and induced H3K9me3 are activated after knockdown of *Parp1* (Fig.

doi:10.6342/NTU201903408

11E, F and J). The result indicates that knockdown of *Parp1* leads to Zscan4 derepression while excessive expression of Zscan4 may activate several genes to suppress hyper-recombination and maintain genome stability.

3-4. PARP1 inhibition in *Terc*$^{+/-}$ ntESCs activated telomere regulation genes

Telomere syndrome is a disease caused by telomerase insufficient and short telomere. The patient suffers from idiopathic pulmonary fibrosis, dyskeratosis congenita, etc (Armanios and Blackburn, 2012). A previous study shows that telomerase haplo-insufficient ntESCs have defect on chondrocyte differentiation (Chang et al., 2019). Since most of the telomere syndrome patient is *Terc* haplo-insufficient, *Terc*$^{+/-}$ ntESCs are used as model, and applied 3-AB to see if the drug can elongate telomere length as the result in wild type ESCs (Fig. 10).

First, by PCR and agarose electrophoresis, the genotyping was performed to make sure ntESCs clones I cultured are *Terc* haplo-insufficient (Fig. 13A). After treated 3-AB for 3 passages, *Terc*$^{+/-}$ ntESCs clones show different result on telomere length (Fig. 13N). Clone#5 and clone#6 shows slightly shorten of telomere length while clone#7 shows significantly increase of telomere length compared to DMSO control (1.25 fold-change compared to DMSO control, Fig. 13N). It is worth noting that in DMSO control groups, clone#7 shows shorter telomere length compared to clone#5 and clone#6 (Fig. 13N). The result suggested that telomere length change after PARP1 inhibition may depend on original telomere length.

Further, by qRT-PCR, I found that PARP1 inhibition increases *Parp1*, *Zscan4* and *Terc* but not *Tert* mRNA expression level (Fig. 13B-E). The result confirmed that

doi:10.6342/NTU201903408

PARP1 inhibits expression of *Zscan4* again. Moreover, the gene involves in derepression of *Zscan4*, increasing of T-SCE and the gene maintain activity of PI3K pathway (*Rtel1, Telo2* and *Tbx3*) showed increasing after PARP1 inhibition in all the 3 clones (Fig. 13K-M). Interestingly, the gene inhibit Zscan4, preventing hyper-recombination or playing a role in generate repressed histone or DNA modification (*Rif1*, *Atrx*, *Suv39h2* and *Dnmt3b*) only shows increase in clone#5 and clone#6 but not Clone#7 (Fig. F-I). In clone#7, the gene inhibits recombination do not increase mRNA expression level (Fig. F-I). The result indicates that PARP1 inhibition has potential to rescue short telomere in *Terc* haplo-insufficient ntESCs. The telomere elongation phenotype in clone#7 may due to increasing of promote recombination and derepressed genes but not inhibition genes. In summary, Parp1 inhibition in $Terc^{+/-}$ ntESCs activated multiple telomere-related genes and further affected telomere length homeostasis (Fig. 13O).

doi:10.6342/NTU201903408

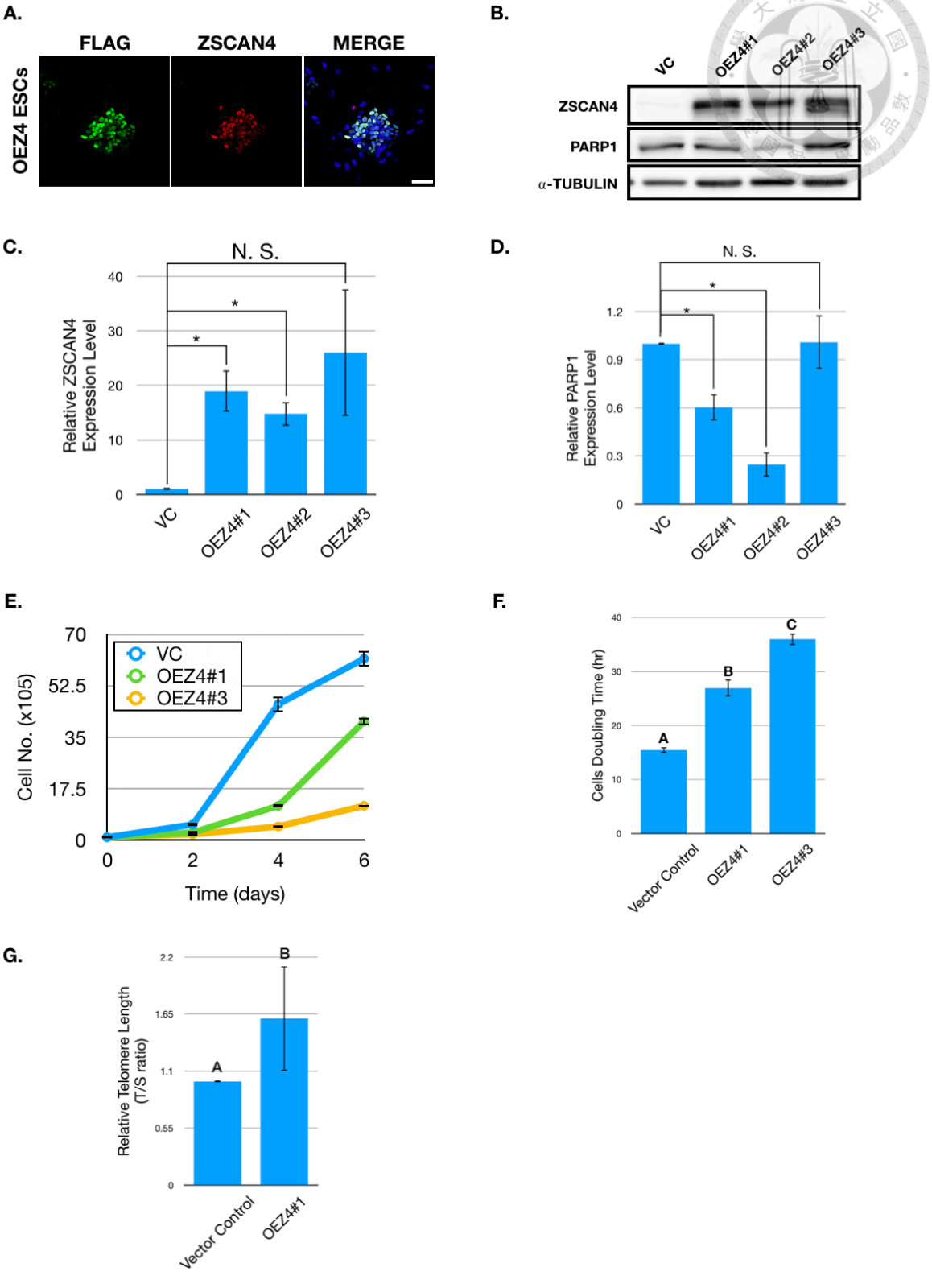

doi:10.6342/NTU201903408

Figure 8. Characteristics of ZSACN4 over-expression ESC clones.

(A) Immunostaining of OEZ4 ESCs by anti-FLAG and anti-ZSCAN4 antibody. Scale bar: 50 μm. (B) Western blot of OEZ4 ESCs. (C-D) Quantification of ZSCAN4 and PARP1 expression level. (E) Growth curves of Zscan4 over-expression ESCs. 100000 cells were seeded on 12 wells dish with 0.1% gelatin coating at day 0. Cell number was counted by hemocytometer. (F) Cell doubling time of OEZ4 ESCs. (G) Relative telomere length of OEZ4 ESCs at passage 8. Data is represented as Mean± SEM. Statistical analysis was performed by unpaired two-tailed Student's t-tests.

doi:10.6342/NTU201903408

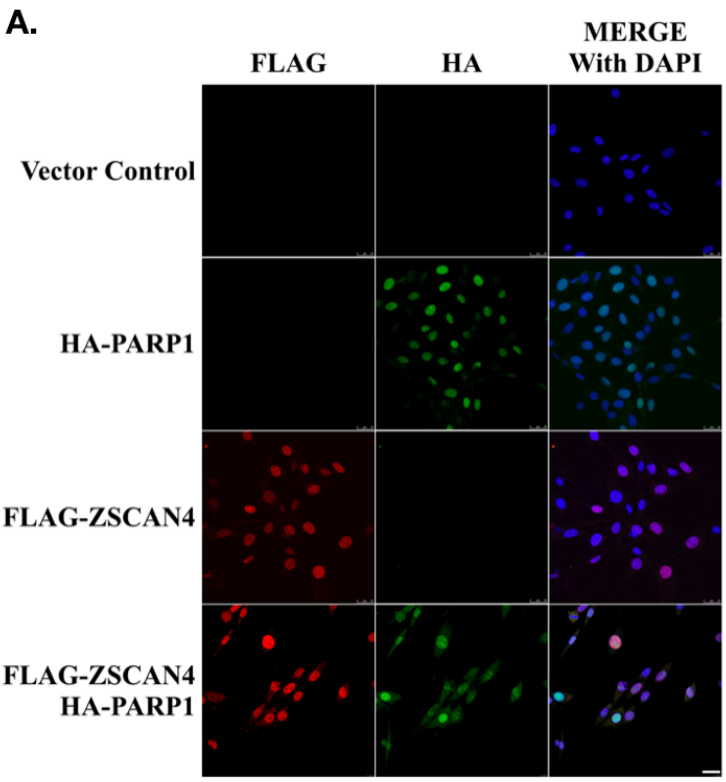

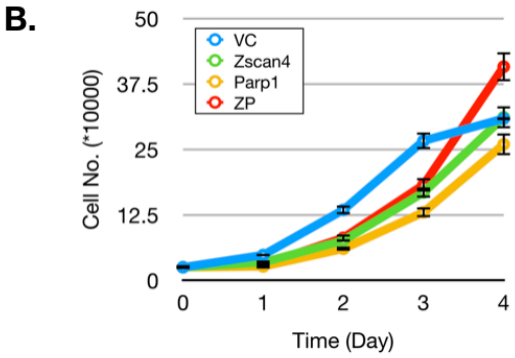

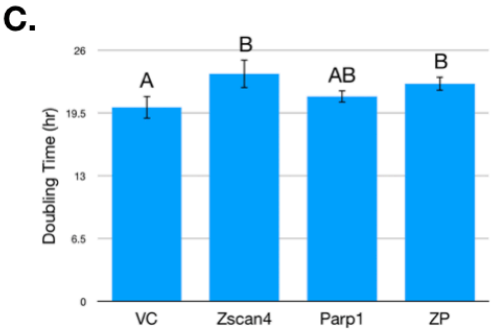

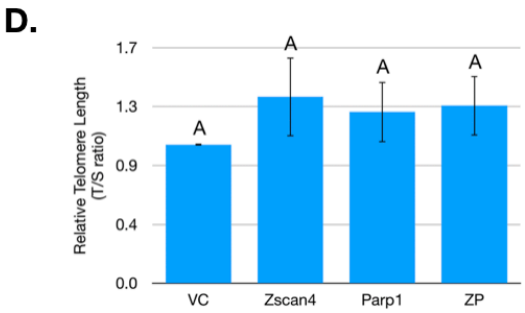

doi:10.6342/NTU201903408

Figure 9. ZSCAN4 and PARP1 do not affect proliferative rate in NIH/3T3 cells.

(A) immunostaining confirms that NIH/3T3 cells expressed ZSCAN4 or/and PARP1. Scale bar: 25 μm. (B) Growth curves of trans-gene NIH/3T3 cells. 25000 cells/ 24 well were seeded in day 0. VC, vector control; ZP, overexpression of both Zscan4 and Parp1. (C) Doubling time of trans-gene NIH/3T3 cells. (D) Relative telomere length of Zscan4 and Parp1 overexpression NIH/3T3 cells. Data is represented as mean±SEM. Statistical analysis was performed by unpaired two-tailed Student's t-tests.

doi:10.6342/NTU201903408

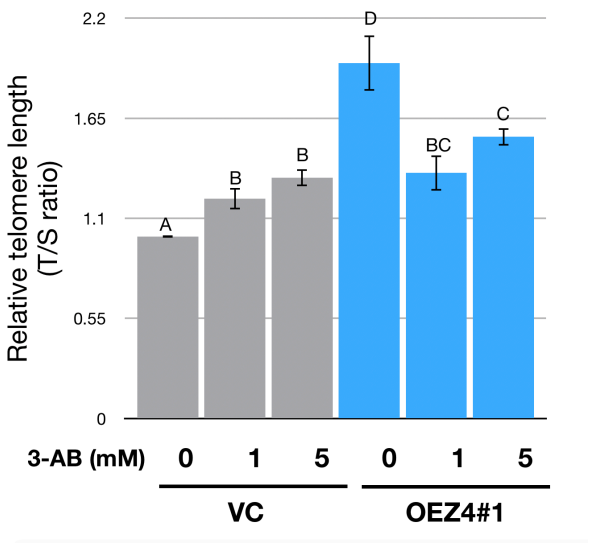

Figure 10. PARP1 involves in *Zscan4* induced telomere elongation.

ES cell lines are treated with different concentration of PARP1 inhibitor, 3-Aminobenzamide in 0.1% DMSO for 3 passages. Relative telomere lengths are normalized with vector control. Data is represented by mean±SEM. VC, Vector control; OEZ4#1, Zscan4 over-expression ESCs clone#1, 0 mM 3-AB treatment means 0.1% DMSO control. Statistical analysis is performed by unpaired two-tailed Student's t-tests.

doi:10.6342/NTU201903408

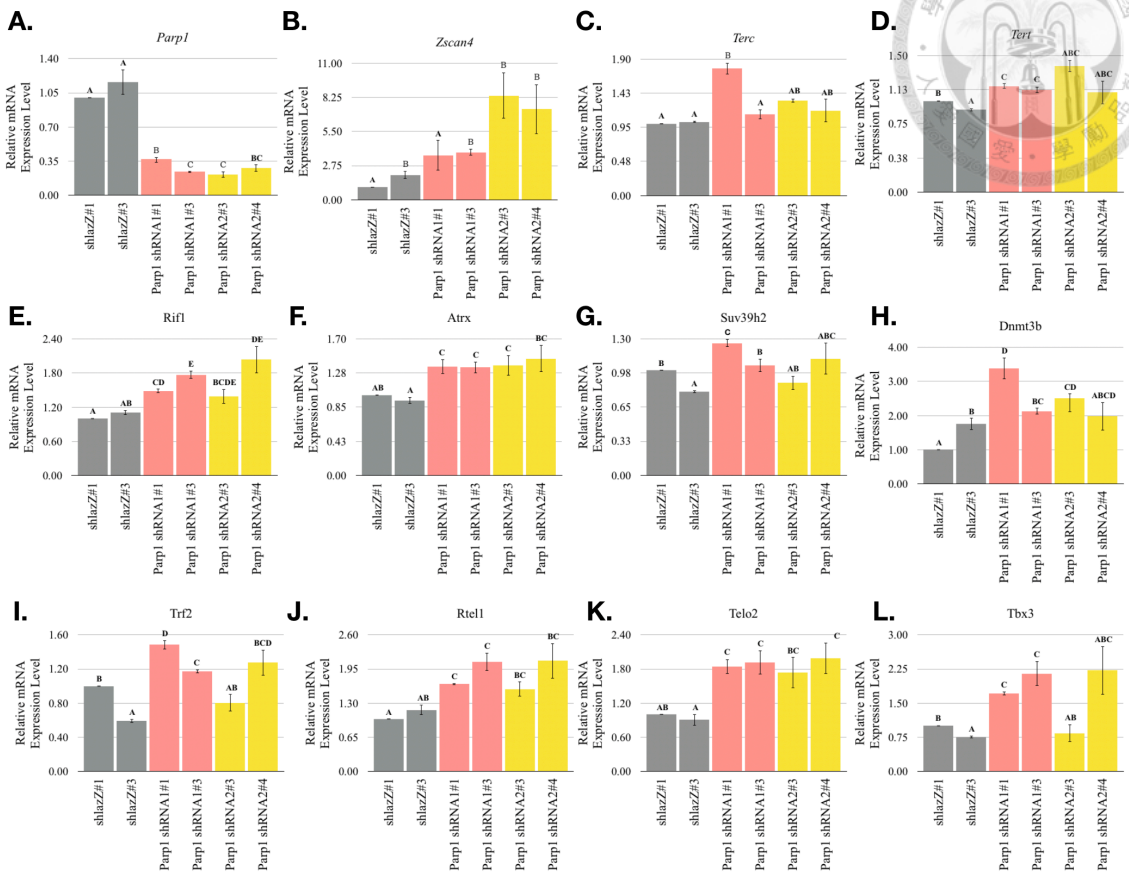

Figure 11. Knockdown *Parp1* affects mRNA expression of telomere-associated genes level in wild type ESCs.

Parp1 is knockdown by 2 different short hairpin RNAs (shRNA) which represented as *Parp1* shRNA#1 (Pink bars) or *Parp1* shRNA#2 (Yellow bars). Knockdown of *lacZ* by shRNA serves as control (Gray bars). Data is represented by mean±SEM. Statistical analysis was performed by unpaired two-tailed Student's t-tests.

doi:10.6342/NTU201903408

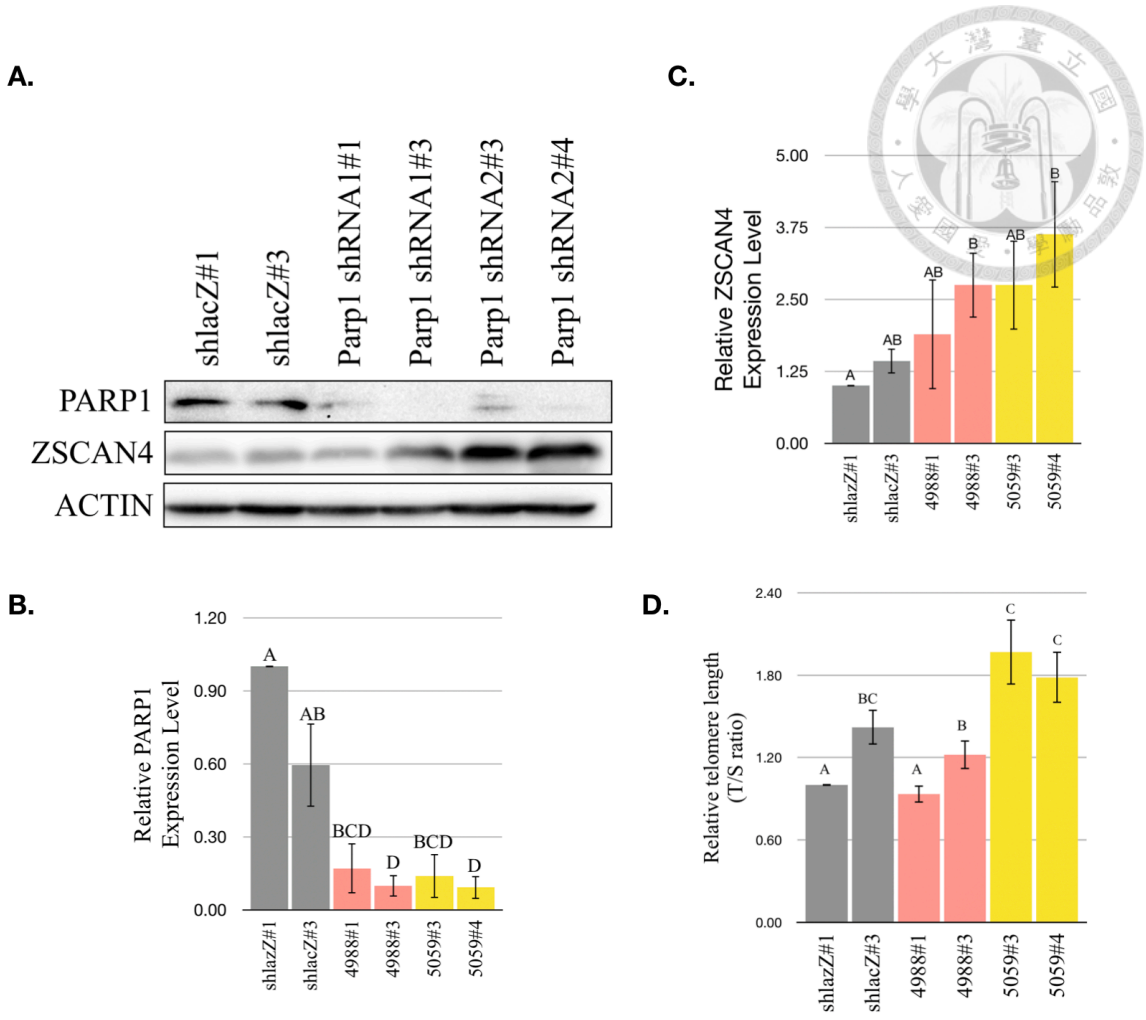

Figure 12. PARP1 inhibits the expression level of *Zscan4* and further telomere elongation in wild type ESCs.

Two different short hairpin RNA of Parp1 are infected into ESCs by lentivirus, respectively. Knockdown lacZ serves as control. ESC clones are picked up after antibiotics selection. (A) Protein expression level of ZSCAN4 and PARP1 are detected by western blot. (B-C) Quantification of relative PARP1 and ZSCAN4 expression levels. Every group is normalized to shlacZ#1. (D) Relative telomere length of shParp1 ESCs. Relative telomere lengths are normalized with shlacZ#1. Data is represented by mean±SEM. VC, Vector control; OEZ4#1, Zscan4 over-expression ESCs clone#1. Statistical analysis is performed by unpaired two-tailed Student's t-tests.

doi:10.6342/NTU201903408

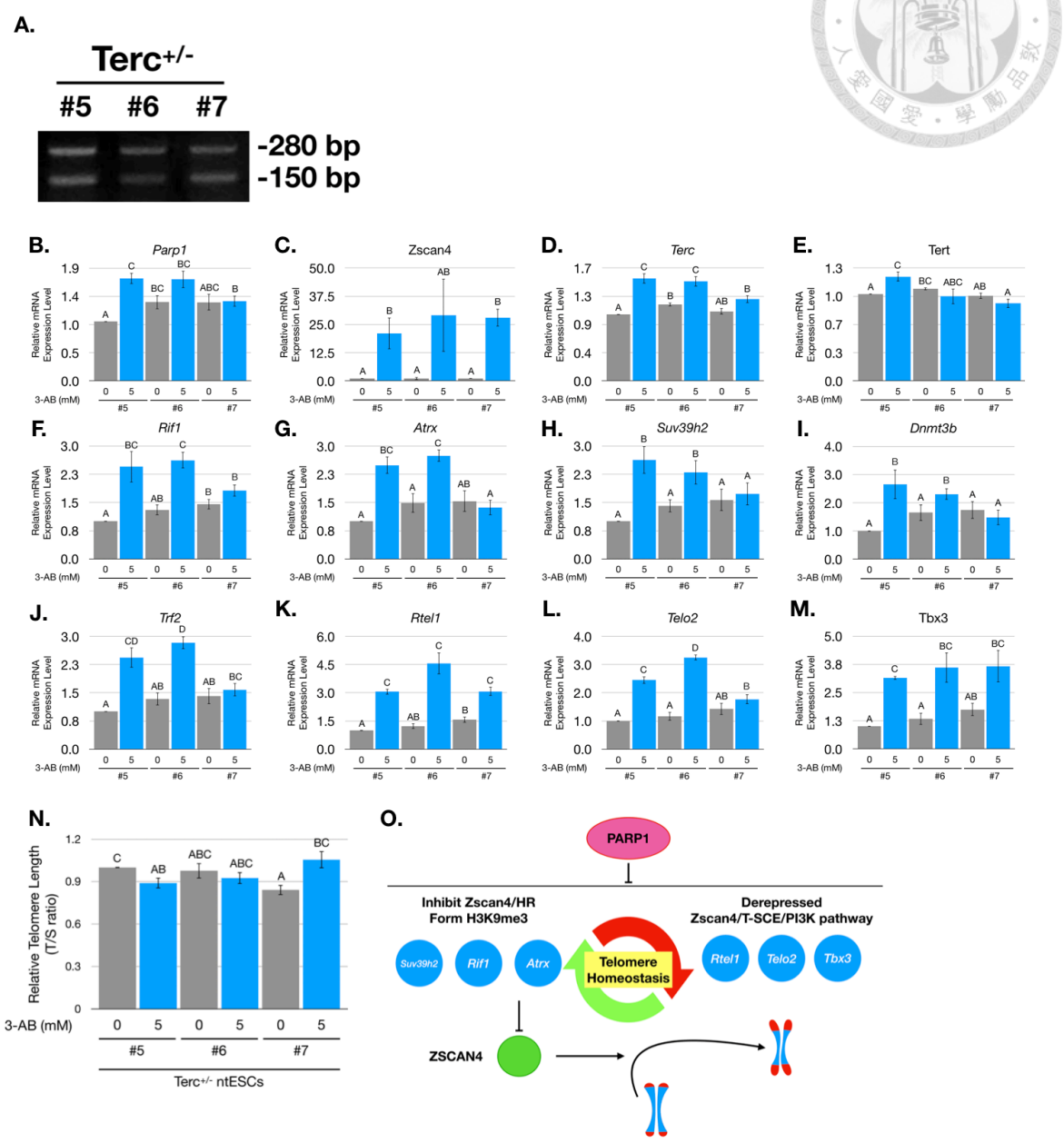

doi:10.6342/NTU201903408

Figure 13. PARP1 inhibits the expression level of Zscan4, telomere-associated genes and telomere length in *Terc*$^{+/-}$ ntESCs.

(A) Genotyping of *Terc*$^{+/-}$ ntESCs. #5-#7 means different *Terc*$^{+/-}$ ntESCs clones. (B-M) Quantification of mRNA expression level of telomere associated genes. Data is normalized with *Terc*$^{+/-}$ ntESCs#5 without 3-AB group. (N) Relative telomere length of Terc$^{+/-}$ ntESCs clones after 3-AB treatment. (O) Illustration of effect of PARP1 in telomere homeostasis. Data is normalized with *Terc*$^{+/-}$ ntESCs#5 without 3-AB group. Data is represented by mean±SEM. Statistical analysis was performed by unpaired two-tailed Student's t-tests.

doi:10.6342/NTU201903408

4. DISCUSSION

OEZ4 ESCs have been generated by multiple research groups (Falco et al., 2007; Zalzman et al., 2010; Dan et al., 2017). *Zscan4* expression certainly leads to telomere lengthening without affects telomerase activity. However, the slower proliferation rate of OEZ4 ESCs have not been reported yet. The possible reason is that *Zscan4* expression ESCs (or the ESCs in 2-cell state) shows translation repressed (Macfarlan et al., 2012; Hung et al., 2013). Lack of suitable protein may result in slower proliferation rate. Further, *Zscan4* expression ESCs (or the ESCs in 2-cell state) also shows hypo-methylation state due to translation block (Eckersley-Maslin et al., 2016). On the other hand, by cell linage trees, *Zscan4* have been reported to be expressed in longer G2/M phase ESCs (Nakai-Futatsugi and Niwa, 2016). Additionally, *Zscan4* overexpression do not show corresponding *Parp1* expression level change. This could be reasonable since in the previous RNA sequencing data, ectopic expression of *Zscan4* affects ~1000 genes while *Parp1* is not on the list (Nishiyama et al., 2009).

PARP inhibition is one way of cancer therapy. From 1970s, 3-AB is the first generation PARP inhibitor, which mimics NAD^+ and is used to apply in cancer therapy (Cepeda et al., 2006). Notably, *Parp1* are often over-expressed in cancer cells. One paper has show that combination of 3-AB with telomerase inhibitor, GRN163L, can shorten telomere length, induce crisis and limit life span of pancreas cancer cells, L3.6pl cells, which lack of ALT mechanism (Burchett et al., 2017). Moreover, *Parp1* knockout mice show shorter telomere length (d'Adda di Fagagna et al., 1999; Piskunova et al., 2008). However, it has also been reported that PARP inhibition can lead to telomere elongation in mouse skin fibroblast cell through activation of ATM pathway (Lee et al., 2015). In the ESCs, two different phenotypes of telomere length after 3-AB treatment

doi:10.6342/NTU201903408

are observed (Fig. 10). In the wild type ESCs, the telomere length shows significance increase after PARP inhibition, which may be caused by derepressed of *Zscan4* according to this study. Another possibility is that PARP1 has been reported to activate *Tert* expression and telomerase activity (Hsieh et al., 2017). Collectively, Parp1 may play multiple roles not only in ZSCAN4-dependent ALT pathway but also in telomerase pathway to regulate telomere length.

Knockdown of gene expression by shRNA is mechanically different than chemical inhibition. By 3-AB, all the PARPs activity are inhibited while the protein is existence which may still occupy the position on DNA or interaction protein. On the other hand, knockdown of *Parp1* by shRNA blocks translation and is theoretically more specific. The knockdown efficiency of *Parp1* in my study is ~80% at both transcription al and translational level which is comparable to another published paper (Hsieh et al., 2017). Two different *Parp1* shRNAs show different telomere elongation effect with similar Parp1 knockdown efficiency (Fig. 12D). The result may be caused by clone specificity while the off-target effect can not be excluded. To further prevent off-target effect, specific Parp1 mutant ESCs (for example: Parp1 E988K for enzyme activity mutant) must be generated to examine (Hsieh et al., 2017). Compared with PARP1 inhibition data, knockdown of *Parp1* by shRNA#2 shows longer telomere length change (1.2- vs. 1.8-fold change, 3-AB vs. *Parp1* shRNA#2 treatment, Fig. 10 and Fig. 12D). The chemical inhibition effect is striking than knockdown of *Parp1*, validating the previous viewpoint (Helleday, 2011; Doksani and de Lange, 2016). On the other hand, *Parp1* deficiency affects several genes expression level. *Zscan4* shows derepression in *Parp1* knockdown ESCs, which is different than published data in facioscapulohumeral Muscular Dystrophy (FSHD) myoblast in human (Sharma et al.,

doi:10.6342/NTU201903408

2016). *DUX4*, which is the activator of *ZSCAN4,* is activated in human FSHD myoblast. It has been found the PARP inhibitor, 3-AB, inhibit *ZSCAN4* in FSHD myoblast (Sharma et al., 2016). The different result may be caused by the different cell types and the pathology of FSHD myoblasts. Moreover, PARP1 has be found to bind on *ZSCAN4* promoter in HEK293T cells by CHIP assay (Lodhi et al., 2014). This data may suggest that PARP1 has ability to inhibit Zscan4 expression. Lastly, several telomere-related genes show up-regulated after knockdown of Parp1 (Fig. 11E-L). The result indicates that *Parp1* plays a role in telomere length regulation. Further, since the gene detected are epigenetic-related, Parp1 may also remodel epigenetic on sub-telomeric and telomere region.

Telomere syndrome patient suffered from short telomere length and incomplete differentiation (Armanios and Blackburn, 2012). In *Terc* haplo-insufficent ntESCs, I observed different telomere length change between clones after PARP inhibition. First, I noticed that between the ntESCs clones elongate telomere or not, there are two major differences. First is whether the gene inhibits *Zscan4* or HR is activated or not (Fig. 13 F-M). Second, the clone with elongated telomere length (Clone#7) has relatively lower telomere length among the 3 clones I tested. The result leads to a question: whether PARP inhibition elongated telomere length depends on original telomere length in $Terc^{+/-}$ ntESCs or depends on the gene inhibit *Zscan4* or HR be activated or not. To address this question, *Terc* knockout ntESCs may also be examined.

doi:10.6342/NTU201903408

GENERAL DISCUSSION

In 2007, *Zscan4* has be found only expressed in 2-cell stage embryo *in vivo* and a subpopulation of ESCs in *in vitro* culture cells (Falco et al., 2007). Three years later, *Zscan4* was found elongate telomere through increasing T-SCE rate (Zalzman et al., 2010). However, the molecular mechanism is still unclear. In this study, I try to uncover mechanisms of *Zscan4* participate in telomere length regulation by investigating the potential ZSCAN4-associated protein, PARP1.

In the first chapter, I uncover the interaction domain between ZSCAN4 and PARP1 by serial co-IP experiments. ZSCAN4 shows interaction with PARP1 through SCAN domain and ZF domain, while PARP1 associated with ZSCAN4 by DB and AM domain. SCAN domain and AM domain are both responsible for holo- or hetero- dimer (Cepeda et al., 2006; Dan et al., 2017), indicating that ZSCAN4 and PARP1 interaction may affect their protein functions. On the other hand, PARP1 has enzyme activity of ADP-ribose polymerization. Whether ZSCAN4 is a potential target of PARP1 needs further investigation. Secondly, by PARP1 inhibition and shRNAs, I discover that PARP1 inhibits Zscan4 expression in mouse ESCs. In the previous study, *Parp1* knockout mice show telomere short (d'Adda di Fagagna et al., 1999). This difference may be caused by the *in vivo* and *in vitro* conditions. Moreover, cellular physiology of ESCs is dramatically different than somatic cells (Boland et al., 2014). These difference lead ESCs to a special location for investigating Zscan4 and telomere length regulation.

In this study, I found PARP1 may play dual roles in *Zscan4* induced telomere elongation: 1) Inhibition of PARP1 lost longer telomere length phenomenon of *Zscan4* over-expression ESCs. The data indicates PARP1 involves in ZSCAN4 induced telomere elongation. 2) Inhibition of PARP1 also activated *Zscan4* and elongated

doi:10.6342/NTU201903408

telomere length in both wild type ESCs and *Terc*$^{+/-}$ ntESCs. Between these 2 roles, whether PARP1 involved in ZSCAN4 elongates telomere length is needed for more investigation.

In future, there are several questions are needed to be addressed: 1) whether ZSCAN4 can be poly ADP-ribosed by PARP1. 2) whether PARP1 binds to *Zscan4* promoter and affects *Zscan4* promoter activity. 3) whether PARP1 inhibition serves as a potential strategy to elongate telomere length. 4) Most importantly, whether PARP1 involves in ZSCAN4 mechanism in telomere elongation.

doi:10.6342/NTU201903408

CONCLUSIONS

In this study, I first confirm the mass spectrum prediction that PARP1 is a ZSCAN4-associated protein. Second, by serial co-IP, I discover the interaction domain of ZSCAN4 and PARP1. SCAN domain of ZSCAN4 interacts with both DB and AM domain of PARP1, while ZF domain of ZSCAN4 associates with only AM domain of PARP1 (FIg. 14). Next, I used PARP inhibitor and *Parp1* shRNA to investigate the interaction between *Zscan4* and *Parp1* in ESCs. Wild type and *Zscan4* over expression ESCs show different phenomenon after PARP inhibition. In wildtype ESCs, the telomere length elongate after PARP inhibition; *Zscan4* over expression ESCs lost the elongated telomere length phenomenon. The result indicated that PARP1 play dual role in telomere homeostasis. Lastly, PARP inhibition in *Terc* haplo-insufficent ntESCs shows 1.25 fold-change of telomere elongation in 1 out of 3 clones I test. Taken together, these data provide the novel ZSCAN4-associated protein for uncover the molecular mechanism of ZSCAN4 in telomere length regulation (Fig. 14).

doi:10.6342/NTU201903408

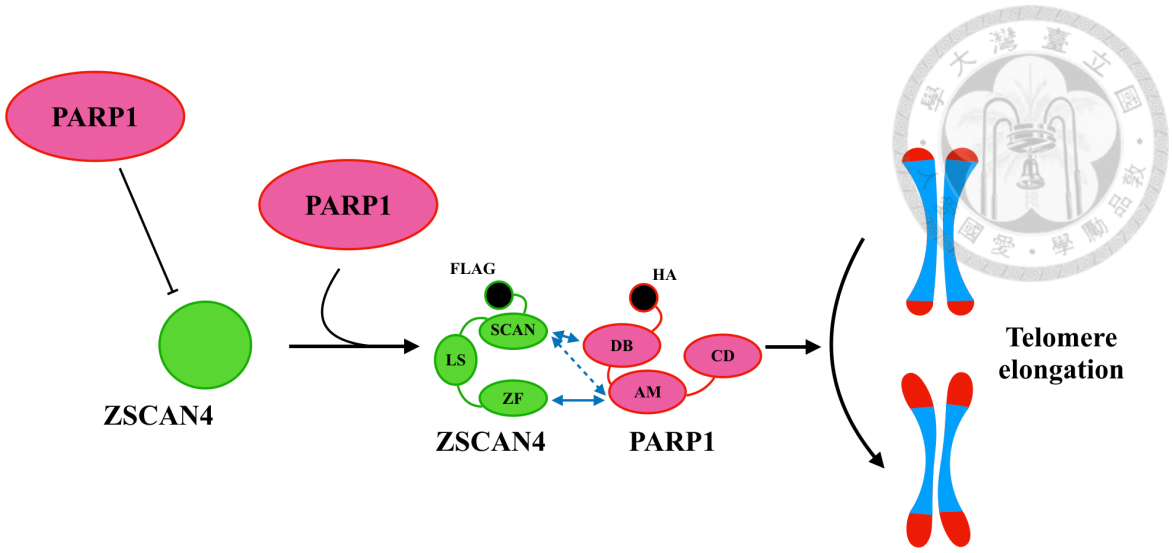

Figure 14. Illustration of PARP1 interacts with ZSCAN4 in telomere homeostasis.

In this study, I found interaction domains of ZSCAN4 and PARP1. PARP1 may play dual roles in ZSCAN4-induced telomere elongation. Pink circle: PARP1. Green circle: ZSCAN4. Dark blue arrow lines mean the interaction domain of PARP1 and ZSCAN4. The solid line means the interaction is stronger. The dotted line means the interaction is weaker. Blue bar with red cap: chromosome and the telomere.

doi:10.6342/NTU201903408

REFERENCES

Aguado, T., F. J. Gutierrez, E. Aix, R. P. Schneider, G. Giovinazzo, M. A. Blasco, and I. Flores. 2017. Telomere Length Defines the Cardiomyocyte Differentiation Potency of Mouse Induced Pluripotent Stem Cells. Stem Cells 35(2):362-373. doi: 10.1002/stem.2497

Akiyama, T., L. Xin, M. Oda, A. A. Sharov, M. Amano, Y. Piao, J. S. Cadet, D. B. Dudekula, Y. Qian, W. Wang, S. B. Ko, and M. S. Ko. 2015. Transient bursts of Zscan4 expression are accompanied by the rapid derepression of heterochromatin in mouse embryonic stem cells. DNA Res 22(5):307-318. doi: 10.1093/dnares/dsv013

Allsopp, R. C., E. Chang, M. Kashefi-Aazam, E. I. Rogaev, M. A. Piatyszek, J. W. Shay, and C. B. Harley. 1995. Telomere shortening is associated with cell division in vitro and in vivo. Exp Cell Res 220(1):194-200. doi: 10.1006/excr.1995.1306

Amano, T., T. Hirata, G. Falco, M. Monti, L. V. Sharova, M. Amano, S. Sheer, H. G. Hoang, Y. Piao, C. A. Stagg, K. Yamamizu, T. Akiyama, and M. S. Ko. 2013. Zscan4 restores the developmental potency of embryonic stem cells. Nat Commun 4:1966. doi: 10.1038/ncomms2966

Armanios, M., and E. H. Blackburn. 2012. The telomere syndromes. Nat Rev Genet 13(10):693-704. doi: 10.1038/nrg3246

Arora, R., and C. M. Azzalin. 2015. Telomere elongation chooses TERRA ALTernatives. RNA Biol 12(9):938-941. doi: 10.1080/15476286.2015.1065374

Audebert, M., B. Salles, and P. Calsou. 2004. Involvement of poly(ADP-ribose) polymerase-1 and XRCC1/DNA ligase III in an alternative route for DNA double-

doi:10.6342/NTU201903408

strand breaks rejoining. J Biol Chem 279(53):55117-55126. doi: 10.1074/jbc.M404524200

Baltimore, D., and D. Smoler. 1971. Primer requirement and template specificity of the DNA polymerase of RNA tumor viruses. Proc Natl Acad Sci U S A 68(7): 1507-1511. doi: 10.1073/pnas.68.7.1507

Blasco, M. A., H. W. Lee, M. P. Hande, E. Samper, P. M. Lansdorp, R. A. DePinho, and C. W. Greider. 1997. Telomere shortening and tumor formation by mouse cells lacking telomerase RNA. Cell 91(1):25-34.

Boesten, D. M., J. M. de Vos-Houben, L. Timmermans, G. J. den Hartog, A. Bast, and G. J. Hageman. 2013. Accelerated aging during chronic oxidative stress: a role for PARP-1. Oxid Med Cell Longev 2013:680414. doi: 10.1155/2013/680414

Boland, M. J., K. L. Nazor, and J. F. Loring. 2014. Epigenetic regulation of pluripotency and differentiation. Circ Res 115(2):311-324. doi: 10.1161/CIRCRESAHA.115.301517

Bryan, T. M., A. Englezou, L. Dalla-Pozza, M. A. Dunham, and R. R. Reddel. 1997. Evidence for an alternative mechanism for maintaining telomere length in human tumors and tumor-derived cell lines. Nat Med 3(11):1271-1274.

Bryan, T. M., A. Englezou, J. Gupta, S. Bacchetti, and R. R. Reddel. 1995. Telomere elongation in immortal human cells without detectable telomerase activity. EMBO J 14(17):4240-4248.

Burchett, K. M., A. Etekpo, S. K. Batra, Y. Yan, and M. M. Ouellette. 2017. Inhibitors of telomerase and poly(ADP-ribose) polymerases synergize to limit the lifespan of pancreatic cancer cells. Oncotarget 8(48):83754-83767. doi: 10.18632/oncotarget.19410

doi:10.6342/NTU201903408

Cepeda, V., M. A. Fuertes, J. Castilla, C. Alonso, C. Quevedo, M. Soto, and J. M. Perez. 2006. Poly(ADP-ribose) polymerase-1 (PARP-1) inhibitors in cancer chemotherapy. Recent Pat Anticancer Drug Discov 1(1):39-53.

Cesare, A. J., and R. R. Reddel. 2010. Alternative lengthening of telomeres: models, mechanisms and implications. Nat Rev Genet 11(5):319-330. doi: 10.1038/nrg2763

Chang, W. F., Y. H. Wu, J. Xu, and L. Y. Sung. 2019. Compromised Chondrocyte Differentiation Capacity in TERC Knockout Mouse Embryonic Stem Cells Derived by Somatic Cell Nuclear Transfer. Int J Mol Sci 20(5)doi: 10.3390/ijms20051236

Cheng, Q., N. Barboule, P. Frit, D. Gomez, O. Bombarde, B. Couderc, G. S. Ren, B. Salles, and P. Calsou. 2011. Ku counteracts mobilization of PARP1 and MRN in chromatin damaged with DNA double-strand breaks. Nucleic Acids Res 39(22): 9605-9619. doi: 10.1093/nar/gkr656

Chiou, S. H., B. H. Jiang, Y. L. Yu, S. J. Chou, P. H. Tsai, W. C. Chang, L. K. Chen, L. H. Chen, Y. Chien, and G. Y. Chiou. 2013. Poly(ADP-ribose) polymerase 1 regulates nuclear reprogramming and promotes iPSC generation without c-Myc. J Exp Med 210(1):85-98. doi: 10.1084/jem.20121044

d'Adda di Fagagna, F., M. P. Hande, W. M. Tong, P. M. Lansdorp, Z. Q. Wang, and S. P. Jackson. 1999. Functions of poly(ADP-ribose) polymerase in controlling telomere length and chromosomal stability. Nat Genet 23(1):76-80. doi: 10.1038/12680

Dan, J., M. Li, J. Yang, J. Li, M. Okuka, X. Ye, and L. Liu. 2013. Roles for Tbx3 in regulation of two-cell state and telomere elongation in mouse ES cells. Sci Rep 3:3492. doi: 10.1038/srep03492

doi:10.6342/NTU201903408

Dan, J., Y. Liu, N. Liu, M. Chiourea, M. Okuka, T. Wu, X. Ye, C. Mou, L. Wang, L. Wang, Y. Yin, J. Yuan, B. Zuo, F. Wang, Z. Li, X. Pan, Z. Yin, L. Chen, D. L. Keefe, S. Gagos, A. Xiao, and L. Liu. 2014. Rif1 maintains telomere length homeostasis of ESCs by mediating heterochromatin silencing. Dev Cell 29(1): 7-19. doi: 10.1016/j.devcel.2014.03.004

Dan, J., P. Rousseau, S. Hardikar, N. Veland, J. Wong, C. Autexier, and T. Chen. 2017. Zscan4 Inhibits Maintenance DNA Methylation to Facilitate Telomere Elongation in Mouse Embryonic Stem Cells. Cell Rep 20(8):1936-1949. doi: 10.1016/j.celrep.2017.07.070

Dan, J., J. Yang, Y. Liu, A. Xiao, and L. Liu. 2015. Roles for Histone Acetylation in Regulation of Telomere Elongation and Two-cell State in Mouse ES Cells. J Cell Physiol 230(10):2337-2344. doi: 10.1002/jcp.24980

Denchi, E. L., and T. de Lange. 2007. Protection of telomeres through independent control of ATM and ATR by TRF2 and POT1. Nature 448(7157):1068-1071. doi: 10.1038/nature06065

Doksani, Y., and T. de Lange. 2016. Telomere-Internal Double-Strand Breaks Are Repaired by Homologous Recombination and PARP1/Lig3-Dependent End-Joining. Cell Rep 17(6):1646-1656. doi: 10.1016/j.celrep.2016.10.008

Eckersley-Maslin, M. A., V. Svensson, C. Krueger, T. M. Stubbs, P. Giehr, F. Krueger, R. J. Miragaia, C. Kyriakopoulos, R. V. Berrens, I. Milagre, J. Walter, S. A. Teichmann, and W. Reik. 2016. MERVL/Zscan4 Network Activation Results in Transient Genome-wide DNA Demethylation of mESCs. Cell Rep 17(1):179-192. doi: 10.1016/j.celrep.2016.08.087

doi:10.6342/NTU201903408

Edelstein, L. C., and T. Collins. 2005. The SCAN domain family of zinc finger transcription factors. Gene 359:1-17. doi: 10.1016/j.gene.2005.06.022

Falco, G., S. L. Lee, I. Stanghellini, U. C. Bassey, T. Hamatani, and M. S. Ko. 2007. Zscan4: a novel gene expressed exclusively in late 2-cell embryos and embryonic stem cells. Dev Biol 307(2):539-550. doi: 10.1016/j.ydbio.2007.05.003

Ferron, S., H. Mira, S. Franco, M. Cano-Jaimez, E. Bellmunt, C. Ramirez, I. Farinas, and M. A. Blasco. 2004. Telomere shortening and chromosomal instability abrogates proliferation of adult but not embryonic neural stem cells. Development 131(16):4059-4070. doi: 10.1242/dev.01215

Frit, P., N. Barboule, Y. Yuan, D. Gomez, and P. Calsou. 2014. Alternative end-joining pathway(s): bricolage at DNA breaks. DNA Repair (Amst) 17:81-97. doi: 10.1016/j.dnarep.2014.02.007

Gao, F., S. W. Kwon, Y. Zhao, and Y. Jin. 2009. PARP1 poly(ADP-ribosyl)ates Sox2 to control Sox2 protein levels and FGF4 expression during embryonic stem cell differentiation. J Biol Chem 284(33):22263-22273. doi: 10.1074/jbc.M109.033118

Gocha, A. R., J. Harris, and J. Groden. 2013. Alternative mechanisms of telomere lengthening: permissive mutations, DNA repair proteins and tumorigenic progression. Mutat Res 743-744:142-150. doi: 10.1016/j.mrfmmm.2012.11.006

Gomez, M., J. Wu, V. Schreiber, J. Dunlap, F. Dantzer, Y. Wang, and Y. Liu. 2006. PARP1 Is a TRF2-associated poly(ADP-ribose)polymerase and protects eroded telomeres. Mol Biol Cell 17(4):1686-1696. doi: 10.1091/mbc.e05-07-0672

Greider, C. W., and E. H. Blackburn. 1985. Identification of a specific telomere terminal transferase activity in Tetrahymena extracts. Cell 43(2 Pt 1):405-413.

doi:10.6342/NTU201903408

Hastings, P. J., J. R. Lupski, S. M. Rosenberg, and G. Ira. 2009. Mechanisms of change in gene copy number. Nat Rev Genet 10(8):551-564. doi: 10.1038/nrg2593

Helleday, T. 2011. The underlying mechanism for the PARP and BRCA synthetic lethality: clearing up the misunderstandings. Mol Oncol 5(4):387-393. doi: 10.1016/j.molonc.2011.07.001

Hirata, T., T. Amano, Y. Nakatake, M. Amano, Y. Piao, H. G. Hoang, and M. S. Ko. 2012. Zscan4 transiently reactivates early embryonic genes during the generation of induced pluripotent stem cells. Sci Rep 2:208. doi: 10.1038/srep00208

Hsieh, M. H., Y. T. Chen, Y. T. Chen, Y. H. Lee, J. Lu, C. L. Chien, H. F. Chen, H. N. Ho, C. J. Yu, Z. Q. Wang, and S. C. Teng. 2017. PARP1 controls KLF4-mediated telomerase expression in stem cells and cancer cells. Nucleic Acids Res 45(18): 10492-10503. doi: 10.1093/nar/gkx683

Huang, J., F. Wang, M. Okuka, N. Liu, G. Ji, X. Ye, B. Zuo, M. Li, P. Liang, W. W. Ge, J. C. Tsibris, D. L. Keefe, and L. Liu. 2011. Association of telomere length with authentic pluripotency of ES/iPS cells. Cell Res 21(5):779-792. doi: 10.1038/cr.2011.16

Hung, S. S., R. C. Wong, A. A. Sharov, Y. Nakatake, H. Yu, and M. S. Ko. 2013. Repression of global protein synthesis by Eif1a-like genes that are expressed specifically in the two-cell embryos and the transient Zscan4-positive state of embryonic stem cells. DNA Res 20(4):391-402. doi: 10.1093/dnares/dst018

Jiang, B. H., W. Y. Chen, H. Y. Li, Y. Chien, W. C. Chang, P. C. Hsieh, P. Wu, C. Y. Chen, H. Y. Song, C. S. Chien, Y. J. Sung, and S. H. Chiou. 2015. CHD1L Regulated PARP1-Driven Pluripotency and Chromatin Remodeling During the

doi:10.6342/NTU201903408

Early-Stage Cell Reprogramming. Stem Cells 33(10):2961-2972. doi: 10.1002/stem.2116

Kosugi, S., M. Hasebe, M. Tomita, and H. Yanagawa. 2009. Systematic identification of cell cycle-dependent yeast nucleocytoplasmic shuttling proteins by prediction of composite motifs. Proc Natl Acad Sci U S A 106(25):10171-10176. doi: 10.1073/pnas.0900604106

Kotter, A., K. Cornils, K. Borgmann, J. Dahm-Daphi, C. Petersen, E. Dikomey, and W. Y. Mansour. 2014. Inhibition of PARP1-dependent end-joining contributes to Olaparib-mediated radiosensitization in tumor cells. Mol Oncol 8(8):1616-1625. doi: 10.1016/j.molonc.2014.06.008

Lazzerini-Denchi, E., and A. Sfeir. 2016. Stop pulling my strings - what telomeres taught us about the DNA damage response. Nat Rev Mol Cell Biol 17(6):364-378. doi: 10.1038/nrm.2016.43

Lee, S. S., C. Bohrson, A. M. Pike, S. J. Wheelan, and C. W. Greider. 2015. ATM Kinase Is Required for Telomere Elongation in Mouse and Human Cells. Cell Rep 13(8):1623-1632. doi: 10.1016/j.celrep.2015.10.035

Li, J. S., J. Miralles Fuste, T. Simavorian, C. Bartocci, J. Tsai, J. Karlseder, and E. Lazzerini Denchi. 2017. TZAP: A telomere-associated protein involved in telomere length control. Science 355(6325):638-641. doi: 10.1126/science.aah6752

Lodhi, N., A. V. Kossenkov, and A. V. Tulin. 2014. Bookmarking promoters in mitotic chromatin: poly(ADP-ribose)polymerase-1 as an epigenetic mark. Nucleic Acids Res 42(11):7028-7038. doi: 10.1093/nar/gku415

doi:10.6342/NTU201903408

Macfarlan, T. S., W. D. Gifford, S. Driscoll, K. Lettieri, H. M. Rowe, D. Bonanomi, A. Firth, O. Singer, D. Trono, and S. L. Pfaff. 2012. Embryonic stem cell potency fluctuates with endogenous retrovirus activity. Nature 487(7405):57-63. doi: 10.1038/nature11244

McVey, M., and S. E. Lee. 2008. MMEJ repair of double-strand breaks (director's cut): deleted sequences and alternative endings. Trends Genet 24(11):529-538. doi: 10.1016/j.tig.2008.08.007

Mehta, A., and J. E. Haber. 2014. Sources of DNA double-strand breaks and models of recombinational DNA repair. Cold Spring Harb Perspect Biol 6(9):a016428. doi: 10.1101/cshperspect.a016428

Min, J., W. E. Wright, and J. W. Shay. 2017. Alternative Lengthening of Telomeres Mediated by Mitotic DNA Synthesis Engages Break-Induced Replication Processes. Mol Cell Biol 37(20)doi: 10.1128/MCB.00226-17

Nakai-Futatsugi, Y., and H. Niwa. 2016. Zscan4 Is Activated after Telomere Shortening in Mouse Embryonic Stem Cells. Stem Cell Reports 6(4):483-495. doi: 10.1016/j.stemcr.2016.02.010

Nishiyama, A., L. Xin, A. A. Sharov, M. Thomas, G. Mowrer, E. Meyers, Y. Piao, S. Mehta, S. Yee, Y. Nakatake, C. Stagg, L. Sharova, L. S. Correa-Cerro, U. Bassey, H. Hoang, E. Kim, R. Tapnio, Y. Qian, D. Dudekula, M. Zalzman, M. Li, G. Falco, H. T. Yang, S. L. Lee, M. Monti, I. Stanghellini, M. N. Islam, R. Nagaraja, I. Goldberg, W. Wang, D. L. Longo, D. Schlessinger, and M. S. Ko. 2009. Uncovering early response of gene regulatory networks in ESCs by systematic induction of transcription factors. Cell Stem Cell 5(4):420-433. doi: 10.1016/j.stem.2009.07.012

doi:10.6342/NTU201903408

Okashita, N., Y. Suwa, O. Nishimura, N. Sakashita, M. Kadota, G. Nagamatsu, M. Kawaguchi, H. Kashida, A. Nakajima, M. Tachibana, and Y. Seki. 2016. PRDM14 Drives OCT3/4 Recruitment via Active Demethylation in the Transition from Primed to Naive Pluripotency. Stem Cell Reports 7(6):1072-1086. doi: 10.1016/j.stemcr.2016.10.007

Ottaviani, D., M. LeCain, and D. Sheer. 2014. The role of microhomology in genomic structural variation. Trends Genet 30(3):85-94. doi: 10.1016/j.tig.2014.01.001

Piskunova, T. S., M. N. Yurova, A. I. Ovsyannikov, A. V. Semenchenko, M. A. Zabezhinski, I. G. Popovich, Z. Q. Wang, and V. N. Anisimov. 2008. Deficiency in Poly(ADP-ribose) Polymerase-1 (PARP-1) Accelerates Aging and Spontaneous Carcinogenesis in Mice. Curr Gerontol Geriatr Res:754190. doi: 10.1155/2008/754190

Roper, S. J., S. Chrysanthou, C. E. Senner, A. Sienerth, S. Gnan, A. Murray, M. Masutani, P. Latos, and M. Hemberger. 2014. ADP-ribosyltransferases Parp1 and Parp7 safeguard pluripotency of ES cells. Nucleic Acids Res 42(14):8914-8927. doi: 10.1093/nar/gku591

Rouleau, M., A. Patel, M. J. Hendzel, S. H. Kaufmann, and G. G. Poirier. 2010. PARP inhibition: PARP1 and beyond. Nat Rev Cancer 10(4):293-301. doi: 10.1038/nrc2812

Sarek, G., P. Marzec, P. Margalef, and S. J. Boulton. 2015. Molecular basis of telomere dysfunction in human genetic diseases. Nat Struct Mol Biol 22(11):867-874. doi: 10.1038/nsmb.3093

doi:10.6342/NTU201903408

Sharma, V., S. N. Pandey, H. Khawaja, K. J. Brown, Y. Hathout, and Y. W. Chen. 2016. PARP1 Differentially Interacts with Promoter region of DUX4 Gene in FSHD Myoblasts. J Genet Syndr Gene Ther 7(4)doi: 10.4172/2157-7412.1000303

Shay, J. W., and S. Bacchetti. 1997. A survey of telomerase activity in human cancer. Eur J Cancer 33(5):787-791. doi: 10.1016/S0959-8049(97)00062-2

Sperka, T., Z. Song, Y. Morita, K. Nalapareddy, L. M. Guachalla, A. Lechel, Y. Begus-Nahrmann, M. D. Burkhalter, M. Mach, F. Schlaudraff, B. Liss, Z. Ju, M. R. Speicher, and K. L. Rudolph. 2011. Puma and p21 represent cooperating checkpoints limiting self-renewal and chromosomal instability of somatic stem cells in response to telomere dysfunction. Nat Cell Biol 14(1):73-79. doi: 10.1038/ncb2388

Storm, M. P., B. Kumpfmueller, H. K. Bone, M. Buchholz, Y. Sanchez Ripoll, J. B. Chaudhuri, H. Niwa, D. Tosh, and M. J. Welham. 2014. Zscan4 is regulated by PI3-kinase and DNA-damaging agents and directly interacts with the transcriptional repressors LSD1 and CtBP2 in mouse embryonic stem cells. PLoS One 9(3):e89821. doi: 10.1371/journal.pone.0089821

Sung, L. Y., W. F. Chang, Q. Zhang, C. C. Liu, J. Y. Liou, C. C. Chang, H. Ou-Yang, R. Guo, H. Fu, W. T. K. Cheng, S. T. Ding, C. M. Chen, M. Okuka, D. L. Keefe, Y. E. Chen, L. Liu, and J. Xu. 2014. Telomere elongation and naive pluripotent stem cells achieved from telomerase haplo-insufficient cells by somatic cell nuclear transfer. Cell Rep 9(5):1603-1609. doi: 10.1016/j.celrep.2014.10.052

Takai, H., R. C. Wang, K. K. Takai, H. Yang, and T. de Lange. 2007. Tel2 regulates the stability of PI3K-related protein kinases. Cell 131(7):1248-1259. doi: 10.1016/j.cell.2007.10.052

doi:10.6342/NTU201903408

Tardat, M., and J. Dejardin. 2018. Telomere chromatin establishment and its maintenance during mammalian development. Chromosoma 127(1):3-18. doi: 10.1007/s00412-017-0656-3

Ulaner, G. A., J. F. Hu, T. H. Vu, L. C. Giudice, and A. R. Hoffman. 1998. Telomerase activity in human development is regulated by human telomerase reverse transcriptase (hTERT) transcription and by alternate splicing of hTERT transcripts. Cancer Res 58(18):4168-4172.

Vilas, C. K., L. E. Emery, E. L. Denchi, and K. M. Miller. 2018. Caught with One's Zinc Fingers in the Genome Integrity Cookie Jar. Trends Genet 34(4):313-325. doi: 10.1016/j.tig.2017.12.011

Williams, A. J., S. C. Blacklow, and T. Collins. 1999. The zinc finger-associated SCAN box is a conserved oligomerization domain. Mol Cell Biol 19(12):8526-8535. doi: 10.1128/mcb.19.12.8526

Yang, G., C. Liu, S. H. Chen, M. A. Kassab, J. D. Hoff, N. G. Walter, and X. Yu. 2018. Super-resolution imaging identifies PARP1 and the Ku complex acting as DNA double-strand break sensors. Nucleic Acids Res 46(7):3446-3457. doi: 10.1093/nar/gky088

Zalzman, M., G. Falco, L. V. Sharova, A. Nishiyama, M. Thomas, S. L. Lee, C. A. Stagg, H. G. Hoang, H. T. Yang, F. E. Indig, R. P. Wersto, and M. S. Ko. 2010. Zscan4 regulates telomere elongation and genomic stability in ES cells. Nature 464(7290):858-863. doi: 10.1038/nature08882

Zhang, J. M., T. Yadav, J. Ouyang, L. Lan, and L. Zou. 2019. Alternative Lengthening of Telomeres through Two Distinct Break-Induced Replication Pathways. Cell Rep 26(4):955-968 e953. doi: 10.1016/j.celrep.2018.12.102

doi:10.6342/NTU201903408

doi:10.6342/NTU201903408